Intratumor childhood vaccine-specific CD4+ T-cell recall coordinates antitumor CD8+ T cells and eosinophils

Michael C Brown ,[1] Georgia M Beasley ,[2] Zachary P McKay,[1] Yuanfan Yang ,[3] Annick Desjardins,[1] Dina M Randazzo,[1] Daniel Landi,[1] David M Ashley,[1] Darell D Bigner,[1] Smita K Nair,[2] Matthias Gromeier[1]

¹Department of Neurosurgery, Duke University School of Medicine, Durham, North Carolina, USA
²Department of Surgery, Duke University School of Medicine, Durham, North Carolina, USA
³Department of Neurosurgery, University of Alabama Division of Neurosurgery, Birmingham, Alabama, USA

Correspondence to
Dr Michael C Brown;
mcb52@duke.edu

ABSTRACT

Background Antitumor mechanisms of CD4+ T cells remain crudely defined, and means to effectively harness CD4+ T-cell help for cancer immunotherapy are lacking. Pre-existing memory CD4+ T cells hold potential to be leveraged for this purpose. Moreover, the role of pre-existing immunity in virotherapy, particularly recombinant poliovirus immunotherapy where childhood polio vaccine specific immunity is ubiquitous, remains unclear. Here we tested the hypothesis that childhood vaccine-specific memory T cells mediate antitumor immunotherapy and contribute to the antitumor efficacy of polio virotherapy.

Methods The impact of polio immunization on polio virotherapy, and the antitumor effects of polio and tetanus recall were tested in syngeneic murine melanoma and breast cancer models. CD8+ T-cell and B-cell knockout, CD4+ T-cell depletion, CD4+ T-cell adoptive transfer, CD40L blockade, assessments of antitumor T-cell immunity, and eosinophil depletion defined antitumor mechanisms of recall antigens. Pan-cancer transcriptome data sets and polio virotherapy clinical trial correlates were used to assess the relevance of these findings in humans.

Results Prior vaccination against poliovirus substantially bolstered the antitumor efficacy of polio virotherapy in mice, and intratumor recall of poliovirus or tetanus immunity delayed tumor growth. Intratumor recall antigens augmented antitumor T-cell function, caused marked tumor infiltration of type 2 innate lymphoid cells and eosinophils, and decreased proportions of regulatory T cells (Tregs). Antitumor effects of recall antigens were mediated by CD4+ T cells, limited by B cells, independent of CD40L, and dependent on eosinophils and CD8+ T cells. An inverse relationship between eosinophil and Treg signatures was observed across The Cancer Genome Atlas (TCGA) cancer types, and eosinophil depletion prevented Treg reductions after polio recall. Pretreatment polio neutralizing antibody titers were higher in patients living longer, and eosinophil levels increased in the majority of patients, after polio virotherapy.

Conclusion Pre-existing anti-polio immunity contributes to the antitumor efficacy of polio virotherapy. This work defines cancer immunotherapy potential of childhood vaccines, reveals their utility to engage CD4+ T-cell help for antitumor CD8+ T cells, and implicates eosinophils as antitumor effectors of CD4+ T cells.

WHAT IS ALREADY KNOWN ON THIS TOPIC

⇒ Intratumor reactivation, or recall, of memory T cells has been shown to mediate antitumor effects in pre-clinical models. Whether pre-existing immunity is an asset to intratumor virotherapy remains contentious, and the antitumor mechanisms of memory T-cell recall remain undefined.

WHAT THIS STUDY ADDS

⇒ Polio and tetanus-specific CD4+ T cells mediate antitumor efficacy after intratumor recall by engaging antitumor functions of eosinophils and potentiating antitumor CD8+ T-cell function; pre-existing, polio-specific CD4+ T cells potentiate the antitumor efficacy a recombinant poliovirus (Lerapolturev) currently being tested in clinical trials.

HOW THIS STUDY MIGHT AFFECT RESEARCH, PRACTICE OR POLICY

⇒ This study implies that intratumor delivery of childhood vaccine associated antigens can mediate cancer immunotherapy and defines eosinophils as key antitumor effectors of memory CD4+ T cells.

INTRODUCTION

Although CD4+ T cells are key mediators of adaptive immune functionality and memory,[1–3] routes to harness their potential for cancer immunotherapy are lacking. Adaptive immune memory enables robust immune responses to previously encountered pathogens. Accordingly, recall responses, that is, activation of adaptive memory cells by cognate antigen, orchestrate localized innate and adaptive inflammation.[4 5] Based upon recent work demonstrating cancer immunotherapy utility of intratumoral antiviral CD8+ T-cell responses,[6 7] we hypothesized that tumor-localized, childhood vaccine-associated CD4+ T-cell recall may engage antitumor functions of CD4+ T cells.

PVSRIPO (now known as 'Lerapolturev'), the live-attenuated poliovirus type 1 (Sabin) vaccine modified with the internal ribosomal

entry site of human rhinovirus type 2,[8] has shown early evidence of efficacy in recurrent glioblastoma (rGBM)[9] and recurrent, non-resectable melanoma[10 11] after intra-tumor (i.t.) administration. Poliovirus (polio) vaccination is part of the standard pediatric immunization schedule worldwide, either with the live attenuated (Sabin), or the inactivated (IPOL) vaccines. The coding sequence of PVSRIPO is identical to the type 1 Sabin vaccine. Pre-existing serum anti-PVSRIPO/polio antibody reactivity was confirmed in all patients receiving PVSRIPO therapy.[9 10 12] Moreover, clinical use of PVSRIPO entails prior boost with trivalent IPOL at least 1 week before its i.t. administration, which caused serum PVSRIPO neutralizing antibody increases in all patients.[9 10] The antitumor effects of polio virotherapy encompass neoplastic cell damage and sublethal viral infection of myeloid cells driving sustained type I interferon (IFN) signaling.[12–15] Anti-polio immune memory likely impedes PVSRIPO replication within the tumor, but may provide an alternate antitumor mechanism of action through i.t. recall of polio vaccine specific T cells.

Using mouse tumor models of melanoma and breast cancer, we demonstrate that pre-existing immunity to polio potentiates the antitumor efficacy of polio virotherapy by engaging antitumor functions of CD4$^+$ T cells. I.t. polio or tetanus recall triggered marked CD4$^+$ T cell, type 2 innate lymphoid cell (ILC2), and eosinophil influx; mediating antitumor efficacy through CD8$^+$ T cells and eosinophils in a CD40L independent manner. In cohorts of patients with rGBM treated with Lerapolturev (PVSRIPO), higher levels of pretreatment polio neutralizing antibodies were associated with longer survival, and peripheral induction of eosinophils were observed in patients with melanoma after i.t. treatment with Lerapolturev. Thus, polio virotherapy and childhood vaccine associated antigens coordinate antitumor type I and II immunity via CD4$^+$ T-cell recall.

MATERIALS AND METHODS

Extended materials and methods are presented in online supplemental information.

Mice, cell lines, viruses, poly(I:C), and in vivo grade antibodies

hCD155-tg C57BL/6 mice were a gift of Satoshi Koike (Tokyo, Japan). Wildtype (wt) (#000664), CD8 knockout (k/o) (#002665), B-cell k/o (#002288), OT-I (#003831), and CD45.1 C57BL/6 mice (#002014) were from The Jackson Laboratory. OT-I and CD45.1 C57BL/6 mice were crossed to generate CD45.1+OT-I mice. B16.F10 (American Type Culture Collection), E0771 (G. Palmer, Duke University, USA), E0771^{hCD155}, B16.F10^{hCD155}, and B16.F10.9^{hCD155}-OVA cells were grown in high-glucose Dulbecco's Modified Eagle Medium (DMEM, Gibco) containing 10% fetal bovine serum (FBS) (Sigma-Aldrich). B16.F10.9^{hCD155}-OVA, B16-F10^{hCD155}, and E0771^{hCD155} cells were previously derived.[12 13] All cell lines were confirmed to be mycoplasma negative. Laboratory grade PVSRIPO,

mouse-adapted PVSRIPO (mRIPO), and UV-inactivated PVSRIPO (UVP) were generated in HeLa cells followed by size exclusion purification of the resultant supernatant as previously described.[12 13] PVSRIPO was used for vaccination; UVP was used to isolate effects of polio capsid (which contains polio vaccine-specific epitopes); mRIPO is a mouse adapted version of PVSRIPO that was used to test the full impact of polio virotherapy in mice. VacciGrade high molecular weight poly(I:C) (InvivoGen) was reconstituted per manufacturer instructions. In vivo grade antibodies to interleukin (IL)-5 (TRFK5) or control (HRPN), CD4 (GK1.5) or control (LTF-2), CD40L (MR-1) or control (#BP0091), and CD40 (FGK4.5) or control (2A3) were from Bio X Cell.

Vaccines, immunizations, and i.t. viral titers

Unless otherwise indicated, vaccines using PVSRIPO (1×10^7 plaque forming units (pfu)/mouse), tetanus toxoid (Tet) (MilliporeSigma; 0.5 µg/mouse), or hemocyanin-keyhole limpet (KLH, Sigma-Aldrich; 100 µg/mouse) were diluted in phosphate buffered saline (PBS) with Alhydrogel (1:1; InvivoGen); 50 µL of vaccine was administered bilaterally in the quadriceps muscles. Combined immunizations of IPOL and Tenivac (Sanofi Pasteur) were administered unilaterally for each vaccine. Vaccine boosts occurred 14 days later. For i.t. viral titers, tumors were harvested, weighed, and mechanically homogenized in 1 mL PBS. Homogenate was tested by plaque assay.[16]

Murine tumor model experiments

For B16 implantations, 2×10^5 cells were implanted subcutaneously into the flank of male and female mice; for E0771 implantations 5×10^5 cells were implanted into the fourth mammary fat pad of female mice. hCD155-tg C57BL/6 mice were used with mRIPO to recapitulate polio virotherapy (active viral replication ± pre-existing immunity); whereas wt C57BL/6 mice, which are non-permissive to polio, were used with UVP to isolate the effects of polio recall. Tumors were treated with either DMEM or PBS (vehicle), mRIPO (1×10^7 pfu), UVP (1×10^8 pre-inactivated pfu), Tet (0.5 µg), and/or poly(I:C) (30 µg) as indicated in figure legends. Treatment groups were randomized by tumor volume (caliper measurements, using the equation L × W × W/2) at the first day of treatment. Mice were euthanized when tumor volume exceeded 1000 mm^3, unless preceded by ulceration (which was infrequent and not associated with any particular treatment), in which case mice were excluded from the study. Group sizes were based on power assessments from pilot experiments, or prior experience.[12] Tumor measurements were performed blinded to the i.t. treatment group starting after the last dose of i.t. therapy/antigen. Mice with outlier starting tumor volume at the time of randomization (1 SD from the mean) were excluded.

Flow cytometry analysis of tumors

Tumors were harvested at time points denoted in figure legends and dissociated in RPMI-1640 media (Thermo Fisher) containing 100 µg/mL Liberase-TM (Sigma-Aldrich) and 10 µg/mL DNAse I (Roche) for 30 min at 37°C, followed by passage through a 70 µM (Olympus Plastics) cell strainer, centrifugation, and washing in PBS. For experiments using Zombie Aqua (BioLegend), cells were stained with Zombie Aqua in PBS (1:500) following manufacturer instructions. Cell suspensions were then incubated with 1:50 mouse TruStain FcX (BioLegend) followed by panel-specific staining in PBS containing 2% FBS. Staining of intracellular transcription factors, cytokines, and granzyme B was accomplished using the Foxp3/Transcription Factor Staining Buffer Set (Thermo Fisher) following manufacturer instructions. See online supplemental information for information about panels and antibodies used. Data were collected on a Fortessa X20 at the Duke Cancer Institute Flow Cytometry Core Facility; FCS files were analyzed using FlowJo V.10 (BD Biosciences). Gating strategies are presented in online supplemental information; isotype controls, fluorescence minus one controls, and comparison to established negative cell populations were used to define positivity.

Clinical trial associated analyses

PVSRIPO neutralization titer assays were performed per the clinical trial protocol,[9] and values for both rGBM clinical trials were used from clinical trial enrollment assays. Phase I rGBM (NCT01491893) polio titers were previously reported[9] and survival was updated as of April 29, 2020; phase II (NCT02986178) survival was updated as of April 27, 2021. Melanoma (NCT03712358)[10 11] clinical trial participant percentages of white blood cells were acquired from clinical complete blood count (CBC) tests.

Statistical analysis and clinical trial cohorts

Assay-specific statistical tests are indicated in the corresponding figure legends. GraphPad Prism V.8 was used to perform statistical analyses. Two-way analysis of variance (ANOVA) was used to assess the difference in tumor growth over time between groups, and ANOVA post hoc testing was used to account for multiple comparisons unless otherwise noted in the figure and/or figure legend. A statistical probability of ($p < 0.05$) was used unless otherwise noted; all p values are two-tailed. All data points reflect individual mice or patients.

RESULTS

Polio immunization potentiates polio virotherapy

We first tested anti-polio antibody production (ie, seroconversion) in mice transgenic for the human poliovirus receptor CD155 (hCD155-tg) on immunization with IPOL or PVSRIPO (to mimic type 1 Sabin) with and without alum adjuvant (Alhydrogel; ALH), part of licensed vaccine formulations (eg, Pentacel, Pediarix, Kinrix).[17] A duration of 45 days between initial immunization and tumor implantation allowed establishment of immunological memory.[18] IPOL achieved limited seroconversion and PVSRIPO immunization elicited a stronger antibody response; ALH bolstered antibody responses to both (online supplemental figure S1A,B). To recapitulate high levels of anti-polio antibodies in patients with cancer,[9] we chose PVSRIPO+ALH (hereafter 'polio') vaccination to determine the role of pre-existing polio immunity in PVSRIPO immunotherapy. Murine tumor models and mice expressing hCD155 were previously developed to permit entry and replication of PVSRIPO, and PVSRIPO was adapted to murine cells to recapitulate viral replication in murine cancer cells (mRIPO).[13 19] In prior studies in polio vaccine naïve, syngeneic mouse tumor models, a single i.t. injection of mRIPO required programmed cell death protein-1 (PD1)/programmed death ligand-1 blockade or tumor expression of the immunogenic ovalbumin (OVA) protein to mediate durable antitumor effects.[12 13] However, i.t. mRIPO mediated durable antitumor efficacy in polio immunized mice in melanoma (B16) and breast (E0771) cancer models, relative to control (KLH) immunized counterparts (figure 1A,B, online supplemental figure S1C). Thus, prior polio immunization bolsters the antitumor efficacy of polio virotherapy.

Polio virotherapy is associated with T-cell inflammation within the tumor.[12 13] mRIPO replication within tumors was substantially reduced in polio immunized mice 2 days and 5 days post-treatment (figure 1C,D), consistent with high neutralizing antibody titers (online supplemental figure S1B). Yet, we observed increased total immune cell density ($CD45.2^+$) in polio immunized mice after mRIPO therapy, explained largely by an influx of conventional $CD4^+$ T cells and myeloid cells ($CD11b^+$, $Ly6G^{Neg}$, $F4/80^+$) (figure 1E, online supplemental figures S2A,S3). Subsequent analysis revealed that the increased $CD11b^+$ myeloid cells in polio immunized mice treated with mRIPO were eosinophils (figure 1F); levels of dendritic cells (DCs) were not significantly altered. Elevated tumor necrosis factor (TNF), granulocyte-macrophage colony-stimulating factor (GM-CSF), IL-1β and IL-17A levels in tumor homogenate and higher IL-4 and IL-5 in explanted tumor draining lymph node (TDLN) cultures from polio immunized mice treated with mRIPO indicated distinct inflammatory responses after mRIPO therapy (online supplemental figure S2B). GM-CSF and IL-5 are known inducers of eosinophil production and recruitment,[20] possibly explaining eosinophil influx in tumors (figure 1F). Conventional $CD4^+$ T cells and eosinophil infiltration in response to mRIPO treatment of polio immunized mice were also observed in a separate model, E0771 (online supplemental figure S2C,D). Thus, pre-existing immunity to polio accentuates inflammatory responses to mRIPO that are associated with enhanced antitumor efficacy.
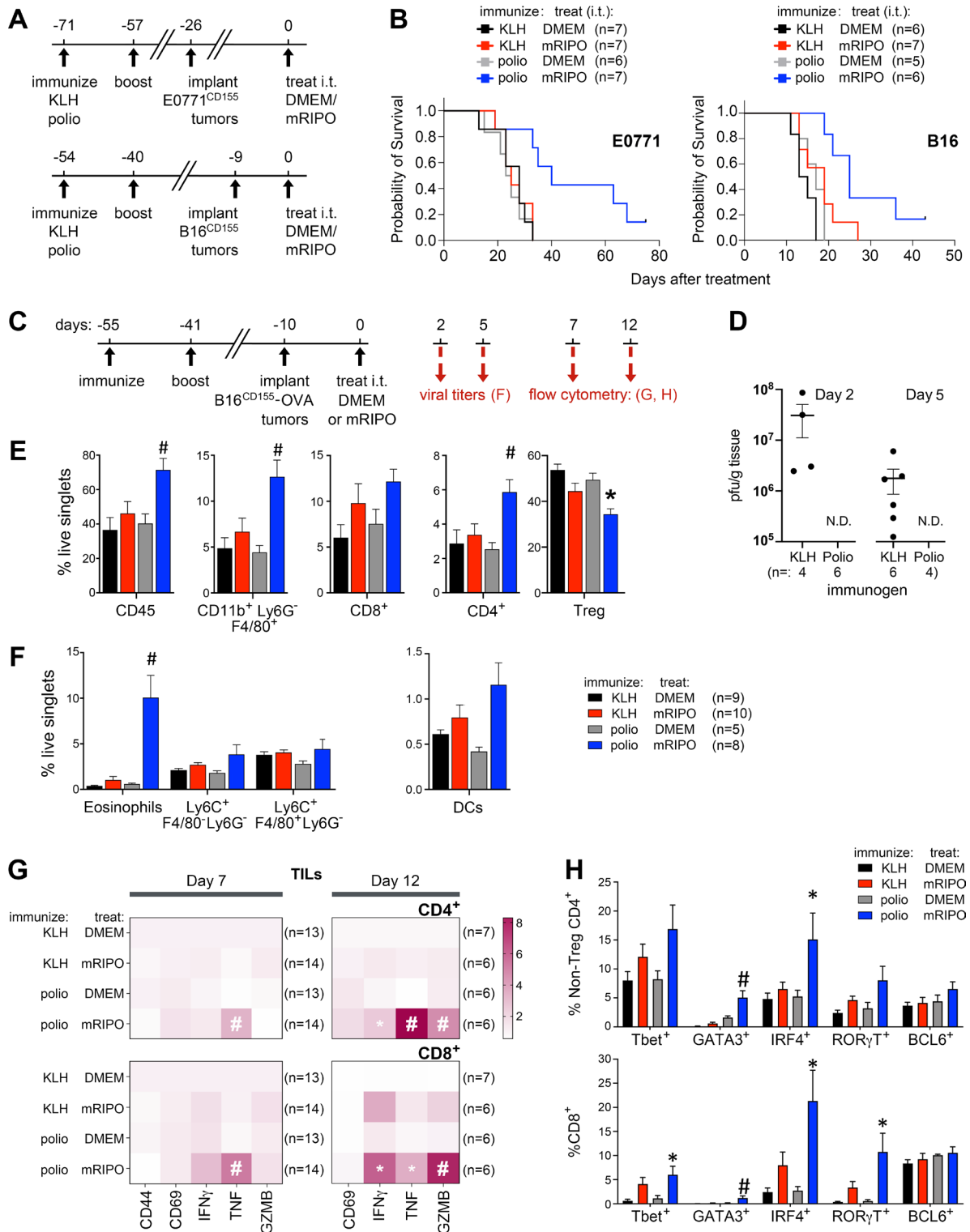
Figure 1 Polio immunization potentiates antitumor and inflammatory efficacy of polio virotherapy. (A) Polio or KLH immunized hCD155-tg mice bearing hCD155-tg B16 or E0771 tumors were treated with DMEM (control) or mRIPO. (B) Survival cut-off was tumor volume >1000 mm³; see online supplemental figure S1C; representative from two experiments. (C) Schema for experiments in D–H. (D) Tumor homogenate viral titers post-mRIPO; N.D., not detected. (E) Flow cytometry analyses of tumors at day 7 (n=13/group mock; n=14/group mRIPO). (F) Flow cytometry analyses for myeloid cells and dendritic cells (DCs: Ly6C^{Neg}, F480^{Neg}, CD11c$^+$, IA/IE$^+$) at day 11. (G) Activation markers in TILs at days 7 and 12; pooled from two experiments; fold mean KLH-DMEM values are shown. (H) TIL transcription factor expression at day 12; same samples as day 12 of (A); representative data of three repeats are shown. See online supplemental figures S1–S4 for extended data. (E–H) Tukey's post hoc test p<0.05 versus mock controls (*) or all other groups (#). Data bars and brackets indicate mean+SEM. mRIPO, mouse adapted PVSRIPO; DMEM, Dulbecco's Modified Eagle Medium; IFN, interferon; i.t., intratumor; KLH, hemocyanin-keyhole limpet; OVA, ovalbumin; TIL, tumor-infiltrating lymphocyte; TNF, tumor necrosis factor.

Augmented T-cell functional phenotypes in polio immunized mice treated with mRIPO

CD8^{+} and CD4^{+} tumor-infiltrating lymphocytes (TILs) in polio vaccinated mice expressed higher levels of intracellular IFN-γ, TNF, and granzyme B post-mRIPO treatment, implying enhanced functional status (figure 1G, online supplemental figure S4). TILs from polio immunized mice treated with mRIPO also exhibited increased expression of the transcription factors Tbet, GATA3, and RORγt; as well as induction of IRF4, a promoter of T-cell activation and function (figure 1H).[21] Expression of the T-cell exhaustion markers PD1 and T cell immunoglobulin and mucin domain-containing protein 3 (TIM3) on CD4^{+} T cells in the tumor and TDLNs of polio vaccinated mice treated with mRIPO were reduced (online supplemental figure S2E). Changes in T-cell activation/ differentiation markers were consistent in the E0771 orthotopic breast cancer model (online supplemental figures S2F,G). Thus, recall responses to polio increase functional phenotypes in TILs after intratumoral polio virotherapy.

Polio and tetanus recall antigens mediate antitumor efficacy

Reovirus-specific memory CD8^{+} T cells directly kill reovirus infected cancer cells during oncolytic reovirus therapy,[22] and tetanus-specific memory CD4^{+} T cells kill cancer cells infected with *Listeria* expressing Tet.[23] Alternatively, inflammatory responses caused by memory T-cell recall in the tumor microenvironment (TME) may also bolster immune surveillance.[6 7] We hypothesized that recall-induced inflammation explained accentuated antitumor efficacy of polio virotherapy in polio vaccinated mice, since viral replication—required for production of viral antigen in tumor cells, oncolysis, and antiviral inflammation[12]—was sharply reduced in polio immunized mice (figure 1D). To probe antitumor effects of polio recall in the TME we used a model devoid of hCD155 (mice and tumors; wt C57BL/6 mice) and treated tumors with UV inactivated PVSRIPO (UVP) to preclude viral infection/replication. We included comparisons with another vaccine-associated recall antigen, Tet, which has been shown to mediate antitumor effects in other studies.[23 24]

I.t. therapy with UVP exerted antitumor efficacy exclusively in polio immunized mice; Tet treatment mediated transient antitumor effects in Tet immunized mice (figure 2A–C, online supplemental file 1). Natural recall responses occur in the presence of a localized innate immune response to pathogen replication. To mimic this, Tet or polio immunized mice were treated with poly(I:C) alone or in combination with UVP or Tet. Both UVP and Tet mediated pronounced antitumor effects in this context (figure 2D). These data reveal that i.t. recall of memory T cells in the TME—independent of the expression/major histocompatibility complex (MHC) presentation of their cognate antigen by malignant cells—mediates antitumor efficacy.

CD4^{+} T cells mediate the antitumor efficacy of recall antigens

To determine which adaptive compartment(s) explain the antitumor efficacy of polio recall responses (independent of viral replication), we compared i.t. treatment with UVP in CD8^{+} T-cell and B-cell k/o mice relative to wt mice (figure 3A). CD4 k/o mice were not tested due to the role of CD4^{+} T cells in enabling both CD8^{+} T-cell and B-cell responses to vaccination. As expected, polio immunization in wt and CD8 k/o mice, but not B-cell k/o mice, led to anti-PVSRIPO antibody production (figure 3B). B16 tumor growth was similar in each genetic context after mock treatment. Relative to wt mice, the antitumor efficacy of UVP in polio immunized mice was limited in CD8 k/o mice at later time points, but was enhanced in B-cell k/o mice (figure 3C; p=0.007 wt vs B-cell k/o UVP treated curves, two-way ANOVA). Moreover, B-cell k/o did not prevent the influx of eosinophils or CD4^{+} TILs (online supplemental figure S6A) associated with polio recall (figure 1). Thus, the antitumor efficacy of polio recall is partially dependent on CD8^{+} T cells, and is limited by B cells.

These observations, along with increased CD4^{+} TILs after mRIPO therapy in polio immunized mice (figure 1E), imply that CD4^{+} T cells dictate the antitumor efficacy of polio recall responses. Thus, we next tested the antitumor effect of polio recall with and without transient CD4^{+} T-cell depletion (figure 3D, starting 1-day pretreatment). Despite robust depletion of CD4^{+} T cells in the TDLN, CD4^{+} T-cell depletion within the tumor was incomplete and preferentially reduced regulatory T cell (Treg) populations, possibly explaining modest antitumor effects and increased CD8^{+} T-cell densities after CD4^{+} T-cell depletion (figure 3D, online supplemental figure S6B). Nonetheless, CD4^{+} T-cell depletion nearly ablated the antitumor efficacy of UVP in polio immunized mice and prevented recruitment of eosinophils in response to UVP (figure 3D); CD4^{+} T-cell depletion also prevented the induction of granzyme B in CD8^{+} T cells after UVP treatment (online supplemental figure S6B). Collectively these findings indicate that the antitumor and inflammatory effects of polio recall are CD4^{+} T-cell dependent. Confirming that polio-specific CD4^{+} T cells are sufficient to potentiate the antitumor efficacy of polio virotherapy (with active viral replication), adoptive transfer of CD4^{+} T cells from spleens of polio immunized mice, but not that of Tet, bolstered the antitumor efficacy of mRIPO (figure 3E, online supplemental figure S6C).

I.t. recall antigen therapy potentiates antitumor CD8^{+} T-cell function

Tumor-specific CD4^{+} T cells were shown to directly kill tumor cells,[25–27] engage cytotoxic innate immune cells,[28 29] and provide help to effector CD8^{+} T cells.[1–3 30] Consistent with the latter, antitumor effects of recall antigens were observed after delivery to the TME (figures 2 and 3), were partially dependent on CD8^{+} T cells (figure 3C), and CD8^{+} TILs had improved polyfunctional phenotypes after mRIPO therapy in polio vaccinated mice (figure 1G).
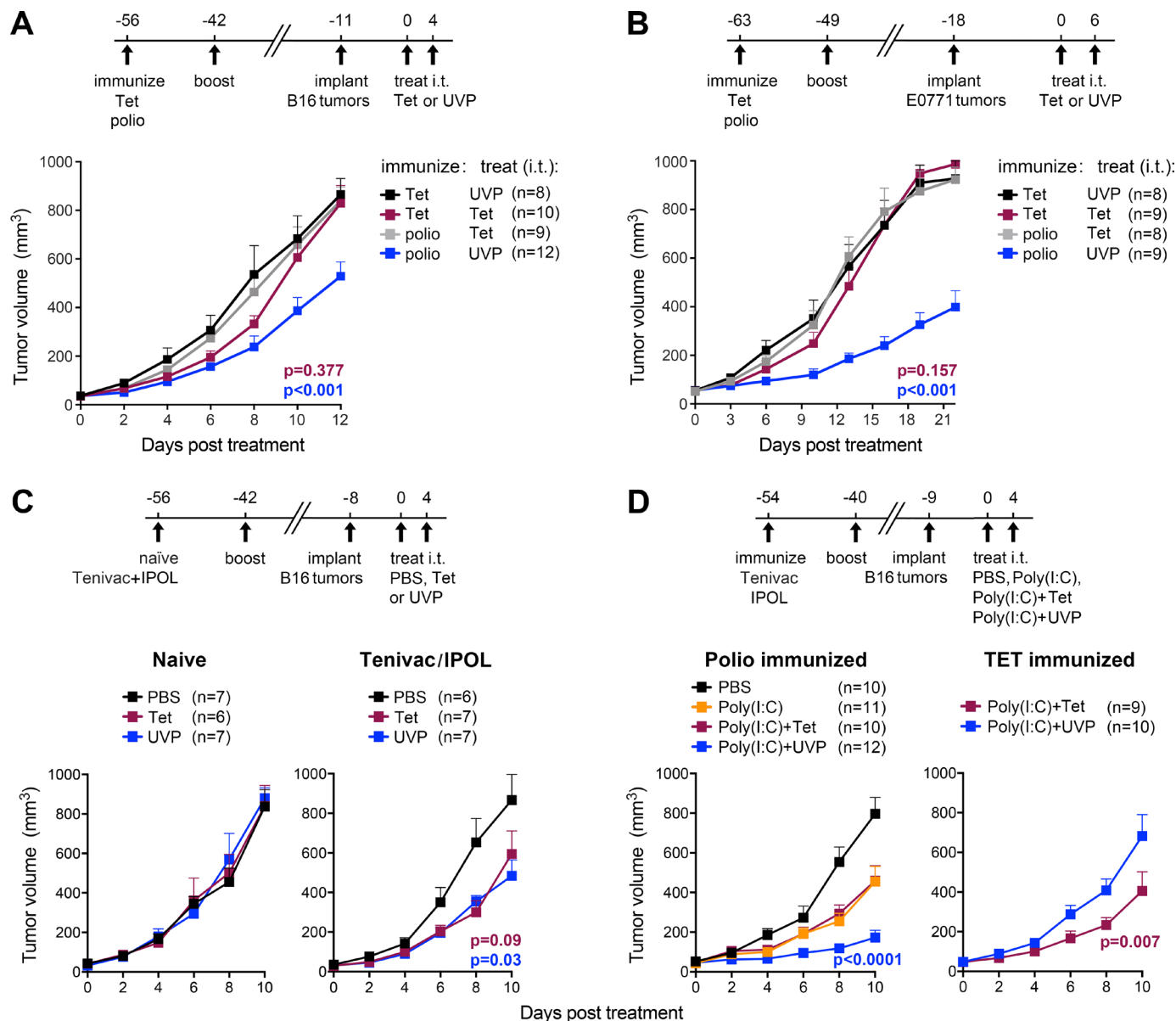
Figure 2 Polio and tetanus recall antigens mediate antitumor efficacy. B16 (A) or E0771 (B) tumor-bearing mice immunized with polio or Tet were treated intratumor with Tet or UV inactivated PVSRIPO (UVP). (C) Age-matched naïve or Tenivac and IPOL immunized mice were treated with PBS, Tet, or UVP. (D) Mice immunized as in (A, B) were treated intratumor with mock, poly(I:C) (30 μg), poly(I:C) + Tet, or poly(I:C) + UVP as shown. (A–D) Mean+SEM from a representative experiment of at least two repeats is shown; asterisks indicate Dunnett's test p<0.05 versus all other groups; online supplemental figure S5 presents extended data. IPOL, inactivated polio vaccine; i.t., intratumor; PBS, phosphate buffered saline; UVP, UV-inactivated PVSRIPO; Tet, tetanus toxoid.

Thus, we next sought to determine if polio (UVP) and Tet recall enhances the function of *antitumor* CD8^{+} T cells. To this end, we adoptively transferred CD45.1^{+} OT-I CD8^{+} T cells (OVA-specific) to polio or Tet vaccinated mice and determined the impact of UVP and Tet-induced recall on B16-OVA OT-I TIL phenotypes (figure 4A). Induction of recall responses in the tumor after UVP or Tet was associated with delayed tumor growth and increased tumor infiltration of endogenous CD45.2^{+} cells, eosinophils, and conventional CD4^{+} T cells; notably, levels of antitumor OT-I T cells were non-significantly increased (figure 4B). However, analysis of tumor infiltrating OT-I

CD8^{+} T cells revealed enhanced granzyme B, TNF, and IFN-γ; and reduced expression of the terminal exhaustion marker TIM3 after polio or Tet recall (figure 4C). Varied Th-associated transcription factor expression in both OT-I and endogenous T cells was observed, including that of GATA3, RORγt, and BCL6 (figure 4C). Transcriptomic analysis of OT-I TILs after polio recall revealed increased expression of granzymes; genes linked with T-cell activation, function, or homeostasis (*Taok3, CD86, CCR5, Egr2, Adgre1, Vdr, IRF4,* and *BCL6*); genes associated with Th1 immunity (*Ptger4, Fgl2*); as well as genes associated with Th2 immunity (*Alox15, Ccl8,* and *GATA3*) (figure 4D,
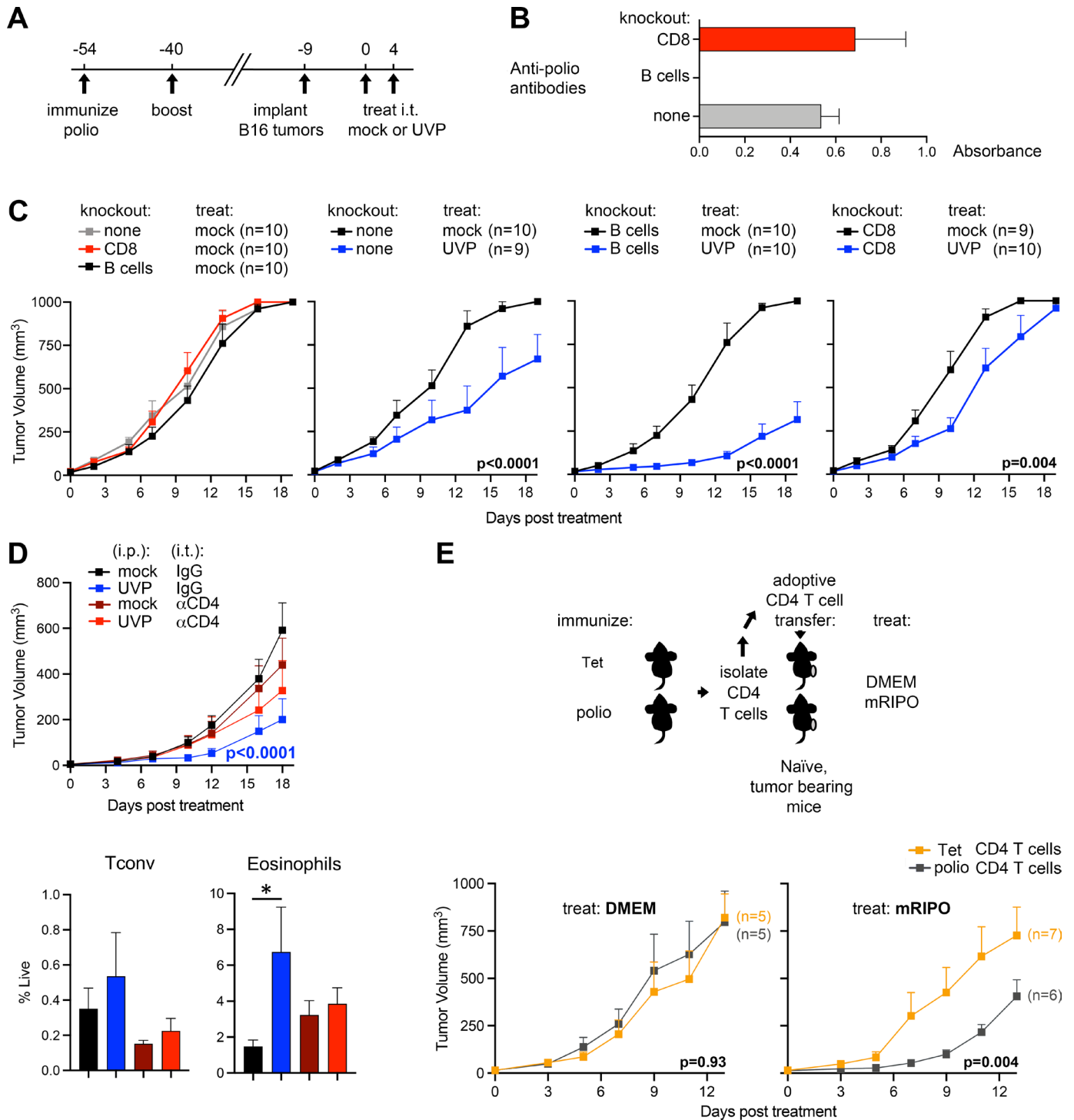
Figure 3 CD4^{+} T cells mediate antitumor efficacy of polio recall. (A) Design for experiments in (B, C). (B) ELISA for anti-polio antibodies in each genetic background at day 0 (n=4/group). (C) Mean tumor volume+SEM after mock treatment (left) or mock versus UVP treatment (right panels) for each genotype context; p values are from two-way analysis of variance (ANOVA) comparison of UVP to the control group. (D) Mice immunized with polio were treated with mock or UVP as in (A), with intraperitoneal (i.p.) injections of IgG (control) or CD4^{+} T-cell depleting antibody (250 µg delivered every 3 days starting at day −1); mean tumor volume+SEM and flow cytometry analysis of tumor infiltrating CD4 T cells and eosinophils are shown; n=9 per group; p value is from a two-way ANOVA comparing UVP IgG versus UVP αCD4; (*) indicates Tukey's post hoc p<0.05. (E) CD4^{+} T cells from spleens of mice immunized with Tet (control) or polio were adoptively transferred to naïve B16 tumor-bearing recipients 1 day-prior to intratumor treatment with DMEM or mRIPO. Mean tumor volume+SEM for mock or mRIPO treated mice for each CD4^{+} T-cell transfer condition; p values are from two-way ANOVA comparison of the two curves shown in each panel. See online supplemental figure S6 for extended data. DMEM, Dulbecco's Modified Eagle Medium; i.t., intratumor; UVP, UV-inactivated PVSRIPO; Tet, tetanus toxoid; mRIPO, mouse adapted PVSRIPO; Tconv, conventional CD4^{+} T cells.
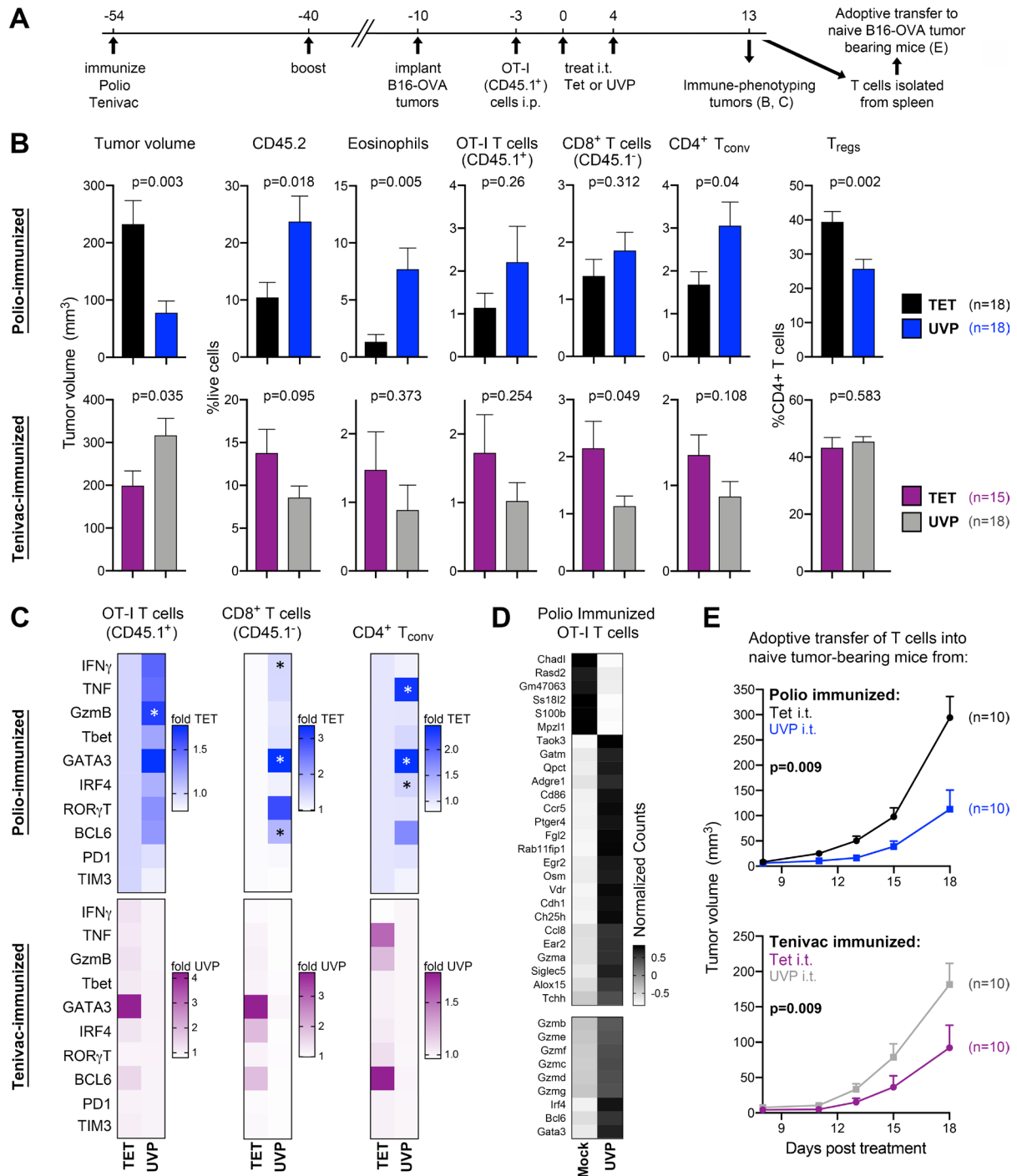
Figure 4 Intratumor recall antigen therapy potentiates antitumor CD8⁺ T-cell function. (A) Polio or Tet (Tenivac) immunized mice were implanted with B16-OVA tumors, followed by adoptive transfer of activated OT-I (CD45.1⁺) cells, and treatment with either Tet or UVP. (B) Tumor volume and flow cytometry analyses of immune cells (B) and TIL subsets (C); online supplemental figure S7 presents gating of OT-I TILs. (D) Transcriptomes of OT-I TILs isolated from polio immunized mice 12 days after treatment (DMEM or UVP) were analyzed. Center and scaled mean normalized counts are shown for transcripts that were significantly different after false discovery rate p value adjustment in two separate experiments (top panel, n=4/group and n=3/group, respectively) or for features relevant to (C) that approached significance in both data sets, including granzymes, IRF4, BCL6, and GATA3 (bottom panel); n=4 replicates/group are shown in heat map. Online supplemental figure S8B,C presents normalized counts for individual samples and extended data. (E) Tumor progression in naïve mice adoptively transferred with T cells from spleens of mice in A–C. Mean tumor volume+SEM is shown; p value is from two-way analysis of variance. All data bars represent mean+SEM; heatmaps in (C) were normalized by fold average of the mismatched antigen control; Tukey's post hoc test p<0.05 relative to all other groups (#) or respective DMEM control (*). (A–C) pooled results from two experiments; data in (E) were repeated twice. DMEM, Dulbecco's Modified Eagle Medium; TIM3, T cell immunoglobulin and mucin domain-containing protein 3; IFN, interferon; i.t., intratumor; OVA, ovalbumin; PD1, programmed cell death protein-1; UVP, UV-inactivated PVSRIPO; Tet, tetanus toxoid; TIL, tumor-infiltrating lymphocytes; TNF, tumor necrosis factor.

online supplemental figure 8C). We confirmed these observations by testing the impact of polio recall on endogenous TRP2-specific (an endogenous B16 antigen) CD8^{+} TILs in B16 tumors without OVA expression. TRP2-specific CD8^{+} TILs exhibited increased granzyme B and reduced TIM3 expression after polio recall in a CD4^{+} T-cell dependent manner (online supplemental figure S9). Together, these data indicate improved cytolytic and functional phenotypes of antitumor T cells after polio recall.

Functionally demonstrating enhanced antitumor T-cell immunity after i.t. recall, T cells isolated from spleens of mice treated with i.t. recall antigen (UVP in polio vaccinated, or Tet in Tenivac vaccinated) delayed tumor growth after transfer to naive recipients (figure 4E). CD4^{+} T-cell help promotes antitumor CD8^{+} T-cell function in part through CD40L signaling to CD40 on antigen presenting cells,[1] but can also help antitumor CD8^{+} T cells independent of CD40L.[31] CD40L blockade did not prevent UVP-induced eosinophil, conventional CD4^{+} T cell, or antitumor OT-I T influx; it also did not antagonize antitumor effects (online supplemental figure S10). In addition, CD40 ligation did not recapitulate eosinophil influx observed after recall antigen therapy (online supplemental figure S10). Thus, i.t. CD4^{+} T-cell recall potentiates the antitumor function of antitumor CD8^{+} T cells in a CD40L independent manner.

Tumor infiltrating eosinophils inversely associate with Tregs in human tumors

Engagement of other antitumor immune effectors via cytokine secretion is a key CD40L-independent mechanism of CD4^{+} T cells.[31 32] I.t polio capsid (UVP) and virotherapy (mRIPO) consistently caused robust i.t. infiltration of eosinophils (figures 1, 3 and 4), in a CD4^{+} T-cell dependent manner (figure 3D). Tumor eosinophil influx associates with immunotherapy response,[33–35] and recent work demonstrated that CD4^{+} T cells enlist antitumor functions of eosinophils after PD1 blockade via IL-5.[36] First, we asked if eosinophil density correlates with that of CD4^{+} T cells or other features in the TME of human tumors by querying a pan-cancer data set from The Cancer Genome Atlas (TCGA).[37] Using CIBERSORT[38] prediction of cell infiltrates,[37] samples from each cancer type were stratified by presence or absence of detected eosinophil gene expression signatures (figure 5A, online supplemental figure S11,12); Testicular Germ Cell Tumors (TGCT) and Uveal Melanoma (UVM) were excluded due to limited cases with eosinophil enrichment (n<3). While limited association of eosinophil presence was observed with CD8^{+} or CD4^{+} T-cell enrichment, eosinophil presence was associated with significantly lower Treg signatures across all cancer types (figure 5A, online supplemental figure S11B,C). Eosinophil presence was associated with longer survival in Low Grade Glioma (LGG), where eosinophil density was also the highest (online supplemental figure S11A), but not in other tumor types (figure 5B, online supplemental figure S11D). Importantly, significant

differences in Treg density on stratification by eosinophil enrichment were observed within several cancer types, with heterogenous relationships between CD4^{+} and CD8^{+} T-cell density (online supplemental figure S12). Notably, eosinophil influx was associated with reduced Treg proportions after polio recall in our studies (figures 1E and 4B, online supplemental figure S2). Together, these data may reflect a role for eosinophils in countering tumor infiltrating Tregs.

Antitumor type II immunity after mRIPO treatment of polio immunized mice

We next sought to determine the significance of eosinophil infiltration after polio recall in mice. Eosinophils are mediators of type II immune responses, which play roles in anti-helminth immunity and allergic inflammation.[39] Eosinophil recruitment can be mediated by other type II immune mediators, including ILC2s, which coordinate Th2 responses through direct interactions with CD4^{+} T cells,[40] express the transcription factor GATA3 and eosinophil promoting cytokine IL-5, but lack T-cell receptor expression. Indeed, GATA3^{+} CD3[Neg] cells increased in tumors of mice after i.t. recall (figure 5C), possibly reflecting ILC2 influx. We next tested how eosinophils impact polio virotherapy (mRIPO) in polio immunized mice, and measured ILC2s directly. Eosinophil depletion (via IL-5 neutralization[41]) mitigated the antitumor effects of mRIPO in B16-OVA[hCD155] bearing, polio immunized mice (figure 5D,E); did not reduce CD4^{+} T-cell influx; but blocked reductions in Treg proportion (figure 5F). Moreover, i.t. polio virotherapy (mRIPO) led to ILC2 influx (figure 5F) and altered ILC2 phenotypes in polio immunized mice, with reduced IL-5 and induced PD1 and granzyme B expression (figure 5G). Aside from its role in controlling eosinophil levels, IL-5 is also critical for B-cell differentiation.[42] However, since the antitumor effects of polio recall are independent of—and possibly countered by—B cells (figure 3C), and because of the consistently robust eosinophil infiltration on polio recall, we conclude that IL-5 neutralization diminishes antitumor effects of polio recall via eosinophil depletion. Collectively, these data demonstrate antitumor roles for eosinophils and recruitment of ILC2s with altered phenotypes after polio recall and imply that eosinophils regulate i.t. Treg densities.

Pre-existing anti-polio antibodies associate with longer survival after Lerapolturev (PVSRIPO) therapy; peripheral eosinophils increase after Lerapolturev

In trials of Lerapolturev in rGBM[9] and melanoma,[10] all patients were confirmed seropositive for anti- PVSRIPO neutralizing antibodies (from polio vaccine cross-reacting antibodies) at the time of enrollment, a feature anticipated to correlate with pre-existing PVSRIPO-specific CD4^{+} T-cell immunity. We queried both phase I (n=61)[9] and II (n=72 at the time of data cut-off) clinical rGBM cohorts for the relationship between pretreatment Lerapolturev neutralizing antibodies and survival. In both
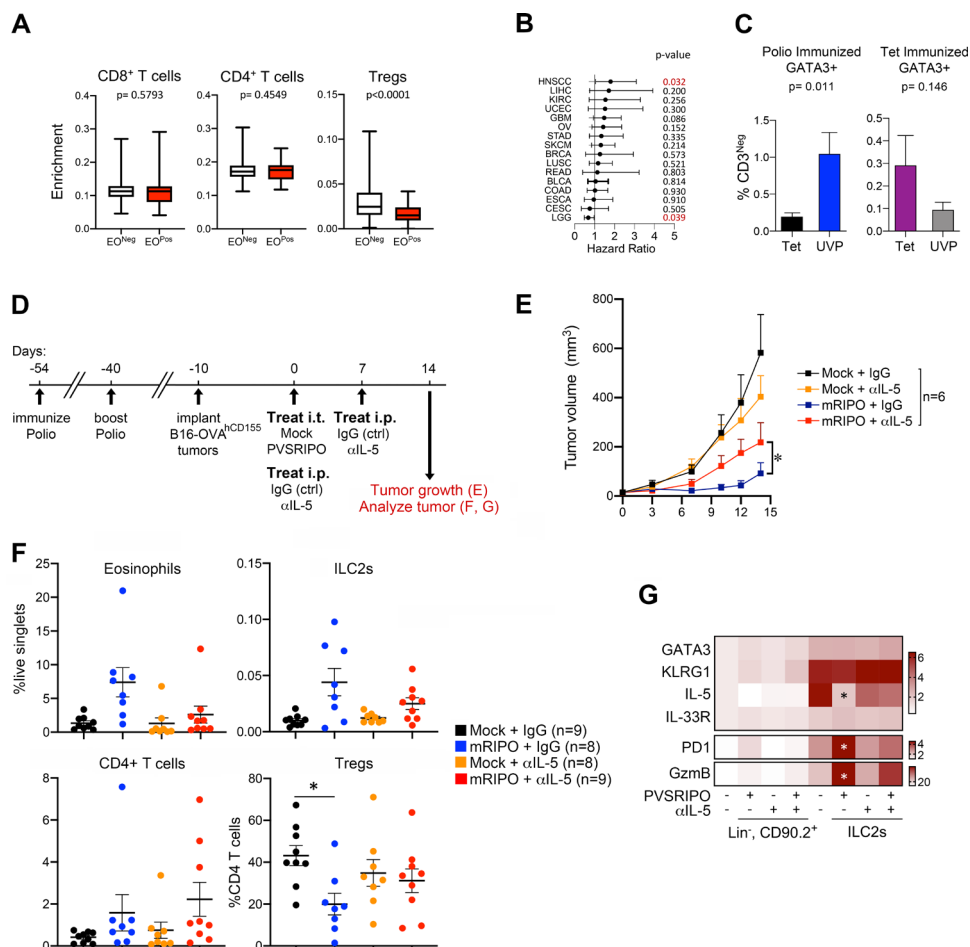
Figure 5 Eosinophils inversely associate with Tregs in human tumors; mRIPO induces antitumor type II immunity in polio immunized mice. (A) CIBERSORT deconvoluted T-cell subsets in The Cancer Genome Atlas cancer types (n=29) stratified by eosinophil status, p values from paired t-test. (B) HRs (survival) ± 95% CIs for eosinophil status by cancer type; cancer types with less than 20 deaths were excluded; p values are from Mantel-Cox log-rank test. (C) Percentage of GATA3+ CD3^{Neg} cells from data in figure 4C, p values are from unpaired t-test. (D) Design for (E–H): polio immunized, B16-OVA^{hCD155} tumor bearing hCD155-transgenic mice were treated with mock or PVSRIPO ± eosinophil depletion (anti-IL-5 or control IgG, 1 mg weekly). Mean tumor volume+SEM (E), eosinophil and ILC2 density in tumors (F), and phenotype of tumor infiltrating ILC2s (lineage^{Neg}CD90$^+$CD127$^+$CD25$^+$) versus lineage negative CD90$^+$ cells for comparison are shown (G). (E) (*)Two-way analysis of variance p<0.05; (F–G) (*)Tukey's post hoc test p<0.05 versus mock+IgG control. Online supplemental figure S11–S13 presents extended data. IL, interleukin; ILC2, type 2 innate lymphoid cell; i.p., intraperitoneal; i.t., intratumor; OVA, ovalbumin; PD1, programmed cell death protein-1; UVP, UV-inactivated PVSRIPO; Tet, tetanus toxoid; Tregs, regulatory T cells; mRIPO, mouse adapted PVSRIPO.

cohorts, patients living >18 months post-Lerapolturev (typical median survival in rGBM is ~9 months)[9 43] had significantly higher pretreatment neutralizing antibody titers (figure 6A,B). To address whether or not type II immune responses may be engaged in patients treated with i.t. polio virotherapy, we analyzed longitudinal CBCs available from a small dose-escalation trial of Lerapolturev in recurrent, unresectable melanoma (phase I, n=12).[10 11] These data revealed increased blood eosinophil levels post-Lerapolturev in 8/12 patients (figure 6C), coinciding with a reduction in neutrophils (10/12 patients). These findings may indicate that pre-existing immunity contributes to the antitumor efficacy of polio virotherapy, and that polio virotherapy induces type II immune responses in patients with cancer.

DISCUSSION

This work reveals cancer immunotherapy potential of tumor-localized CD4$^+$ T-cell recall. CD4$^+$ T-cell help is key for generating fully functional antitumor CD8$^+$ T-cell immunity[1 44] and long-term memory.[2 45] Antitumor CD8$^+$ T cells exhibited greater polyfunctional phenotypes after recall, adoptive T-cell transfer from recall antigen treated mice delayed tumor growth in naïve recipients, and UVP antitumor effects were blunted in polio immunized mice lacking CD8$^+$ T cells. This indicates provision of CD4$^+$ T-cell help to antitumor CD8$^+$ T cells. Indeed, CD4$^+$ T-cell help is linked with exhaustion marker downregulation, elevated TNF/IFN-γ/granzyme B expression, and Tbet/IRF4 induction in 'helped' effector T cells,[3] all of which occurred with polio virotherapy in immunized
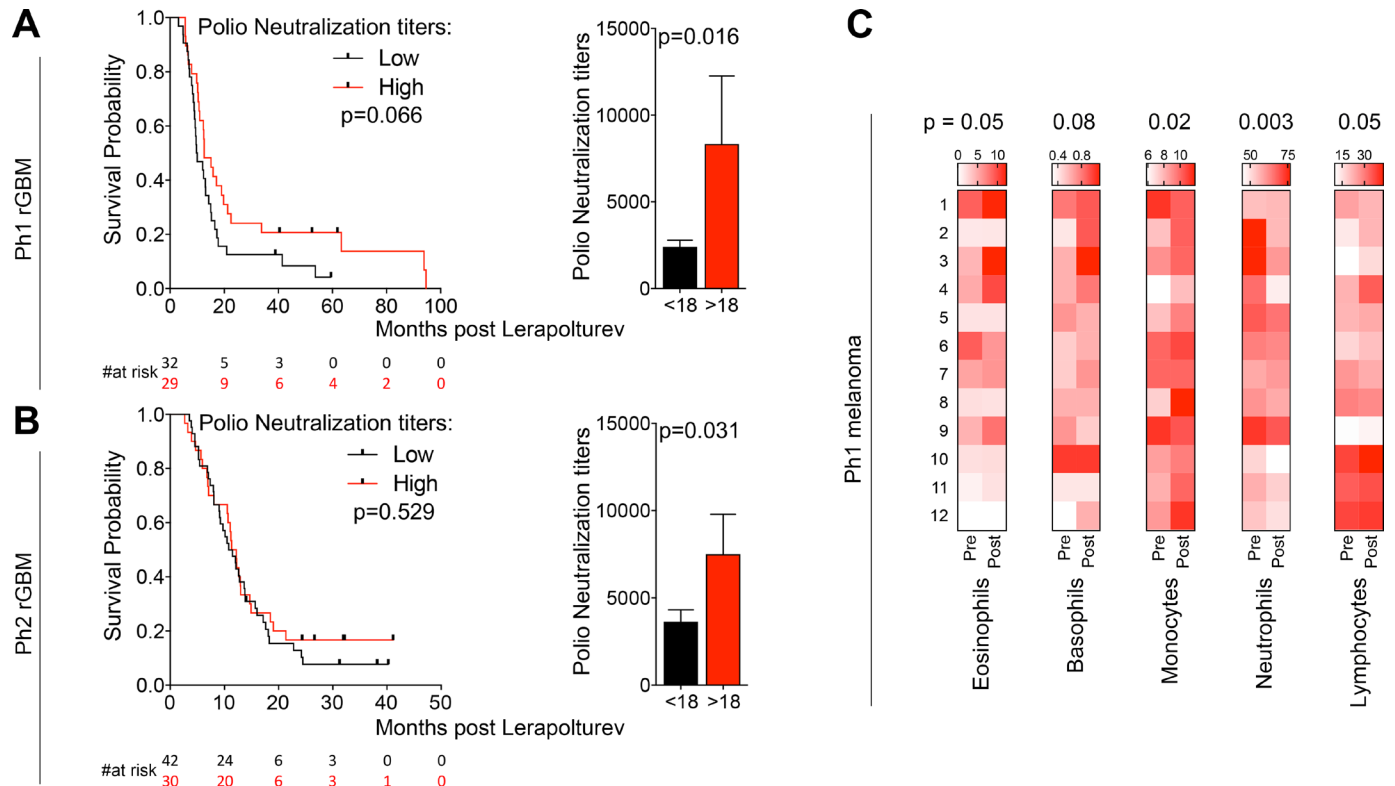
Figure 6 Pre-existing anti-polio antibodies associate with longer survival after Lerapolturev (PVSRIPO) therapy; peripheral eosinophils increase after Lerapolturev. (A, B) Pretreatment Lerapolturev serum neutralization titers were measured in recurrent glioblastoma (rGBM) phase I (A, Ph1, NCT01491893) and phase II (B, Ph2, NCT02986178) trials. Survival after separation by median neutralization titer (1:2000), alongside mean+SEM titer for patients surviving <vs> 18 months after Lerapolturev in the phase I (A) and phase II (B) trials. (A, B) Kaplan-Meier p values are from Mantel-Cox log-rank test; bar graph p values are from unpaired t-test. (C) Percentage of indicated cell types out of total white blood cells at the time of Lerapolturev administration ('pre') and follow-up ('post', 9–11 days after treatment) for all (n=12) patients treated in the phase I melanoma clinical trial (NCT03712358); p values above heatmap are from paired Wilcoxon test.

mice. Such T-cell help is likely multifaceted, including 'licensing' DCs; CD4+ T-cell secretion of cytokines (eg, IL-21, IFN-γ); TME reprogramming; or through positive effects of recruited eosinophils on CD8+ T-cell immune surveillance.[36][46] Possibly due to the activity of polio neutralizing antibodies limiting CD4+ T-cell activation by reducing recall antigen availability or persistence, B cells were counterproductive to antitumor effects of polio recall.

Polio recall consistently mediated stronger antitumor and inflammatory responses than that of Tet in our studies. One possibility is that this is due to differences in the intensity and/or quality of pre-existing immunity induced after polio versus Tet vaccination in our model systems. In support of this possibility, antitumor effects of Tet and UVP were similar when mice were immunized with clinical grade IPOL vaccine (figure 2C), which induced weaker anti-polio immunity than the polio immunization strategy (PVSRIPO+ALH) used for other experiments in our study (online supplemental figure S1B). However, it is also well established that the nature of antigen (eg, epitope density, which is likely higher in the polio capsid) can influence adaptive immune responses.[47][48]

The antitumor efficacy of polio recall only partially depended on CD8+ T cells. Recall antigen therapy caused eosinophil and ILC2 influx, and eosinophil depletion decreased antitumor effects in polio immunized mice treated with mRIPO. Highlighting the importance of context, both eosinophils and ILC2s were also shown to mediate protumorigenic effects.[49][50] In asthma, CD4+ T cells recruit eosinophils[51] via ILC2s.[52] ILC2s express MHC class II and propagate Th2 responses in helminth infections.[40] In cancer, tumor eosinophil infiltration is linked with immunotherapy response,[33][34] eosinophils were shown to support CD8+ T-cell immune surveillance,[46] and ILC2s contribute to anti-PD1 antitumor efficacy.[35][53] Our work indicates that antitumor functions of eosinophils, and possibly that of ILC2s, can be engaged by CD4+ T cells. How CD4+ T-cell recall recruits eosinophils to the tumor remains to be fully determined, however, recent work provides a potential explanation by showing that during PD1 blockade IL-5 secretion by CD4+ T cells induces expansion of eosinophils and i.t. recruitment.[36] Moreover, cytokine analysis of tumor homogenates and TDLN explants after polio virotherapy also revealed increased eosinophil promoting GM-CSF and IL-5 in polio immunized mice (online supplemental figure S2B).

We also discovered an inverse relationship between tumor eosinophil influx and Treg density in human tumors, and recall antigen therapy led to decreased proportions of Tregs that covaried with eosinophil influx, implying a reciprocal role of eosinophils in controlling CD4^{+} T-cell biology. Determining precisely how eosinophils mediate antitumor effects after CD4^{+} T-cell recall, and whether ILC2s contribute to this process requires further study. Differences in eosinophil density alone does not appear to be prognostic in most cancer types, with potential exception of LGG, where eosinophil levels were also the highest among all other tumor types. Interestingly, a negative correlation between peripheral eosinophils and glioma grade has been reported[54]; and respiratory allergies and atopy associate with lower glioma incidence.[55]

We used Th2 polarizing vaccination strategies, consistent with the clinical use of polio and tetanus vaccines, to decipher antitumor potential of CD4^{+} T-cell recall. While—canonically—Th1/Tc1, Th2/Tc2, and Th17/Tc17 polarizations are mutually exclusive, recall antigen therapy in this context produced Th1 (CD8^{+} T-cell engagement, Tbet/IFN-γ expression in CD4^{+} T cells); Th2 (eosinophil/ILC2 recruitment, GATA3 expression in CD4^{+} T cells); and to a lesser extent, Th17 (RORγt expression in CD4^{+}/CD8^{+} T cells) polarizing features. These data add to mounting evidence that diverse CD4^{+} T-cell polarizations, beyond that of Th1, can generate compatible and productive antitumor immune responses.[56–58]

Our work shows that, while pre-existing immunity limits viral replication within the tumor, it enhances the antitumor efficacy of polio virotherapy. A limitation of this work is that it was performed in murine systems that do not capture the heterogeneity of either polio/Tet memory CD4^{+} T-cell responses or the TME in humans. Moreover, due to the rapid growth of tumor models employed, tumors were relatively small at the time of treatment initiation. Nonetheless, suggesting applicability of our observations to humans, pretreatment polio neutralizing antibody titers were higher in patients with rGBM that lived longer after polio virotherapy, and blood eosinophil levels increased in the majority of patients with melanoma (8/12) after i.t. treatment with polio virotherapy (Lerapolturev). As a caveat, higher neutralizing polio antibody titers may reflect superior immune functional status. While we cannot exclude this possibility, these data at minimum reveal that pre-existing immunity does not preclude successful polio virotherapy in patients. Our observations also imply that multiple dosing of Lerapolturev may be warranted to accentuate antitumor effects of polio recall. Indeed, responses in patients with melanoma treated with Lerapolturev clustered in the cohort with the highest number of i.t. treatments.[10]

Given the eminent importance of CD4^{+} T cells in cancer immunotherapy,[1 32] growing efforts aim to leverage CD4^{+} T-cell help within tumors, for example, with CD40 agonistic antibodies,[59] or with peptide vaccines including MHC class II epitopes[44] that prime neoantigen specific CD4^{+} and CD8^{+} T cells.[60] Our work uncovers the potential of harnessing childhood vaccine-specific memory CD4^{+} T cells to engage multifaceted antitumor mechanisms of CD4^{+} T cells.

ORCID iDs
Michael C Brown http://orcid.org/0000-0002-3957-1164
Georgia M Beasley http://orcid.org/0000-0001-6387-9030
Yuanfan Yang http://orcid.org/0000-0003-1581-451X

REFERENCES
1 Borst J, Ahrends T, Bąbała N, et al. Cd4+ T cell help in cancer immunology and immunotherapy. *Nat Rev Immunol* 2018;18:635–47.
2 Ahrends T, Busselaar J, Severson TM, et al. Cd4+ T cell help creates memory CD8+ T cells with innate and help-independent recall capacities. *Nat Commun* 2019;10:5531.
3 Ahrends T, Spanjaard A, Pilzecker B, et al. CD4+ t cell help confers a cytotoxic t cell effector program including coinhibitory receptor downregulation and increased tissue invasiveness. *Immunity* 2017;47:848–61.
4 Schenkel JM, Fraser KA, Beura LK, et al. T cell memory. resident memory CD8 T cells trigger protective innate and adaptive immune responses. *Science* 2014;346:98–101.
5 Ariotti S, Hogenbirk MA, Dijkgraaf FE, et al. T cell memory. skin-resident memory cd8+t cells trigger a state of tissue-wide pathogen alert . *Science* 2014;346:101–5.

6 Rosato PC, Wijeyesinghe S, Stolley JM, *et al*. Virus-specific memory t cells populate tumors and can be repurposed for tumor immunotherapy. *Nat Commun* 2019;10:567.

7 Çuburu N, Bialkowski L, Pontejo SM, *et al*. Harnessing anti-cytomegalovirus immunity for local immunotherapy against solid tumors. *Proc Natl Acad Sci U S A* 2022;119:e2116738119.

8 Gromeier M, Lachmann S, Rosenfeld MR, *et al*. Intergeneric poliovirus recombinants for the treatment of malignant glioma. *Proc Natl Acad Sci U S A* 2000;97:6803–8.

9 Desjardins A, Gromeier M, Herndon JE 2nd, *et al*. Recurrent glioblastoma treated with recombinant poliovirus. *N Engl J Med* 2018;379:150–61.

10 Beasley GM, Nair SK, Farrow NE, *et al*. Phase I trial of intratumoral PVSRIPO in patients with unresectable, treatment-refractory melanoma. *J Immunother Cancer* 2021;9:e002203.

11 Beasley GM, Brown MC, Farrow NE, *et al*. Multimodality analysis confers a prognostic benefit of a T-cell infiltrated tumor microenvironment and peripheral immune status in patients with melanoma. *J Immunother Cancer* 2022;10:e005052.

12 Brown MC, Mosaheb MM, Mohme M, *et al*. Viral infection of cells within the tumor microenvironment mediates antitumor immunotherapy via selective tbk1-irf3 signaling. *Nat Commun* 2021;12:1858.

13 Brown MC, Holl EK, Boczkowski D, *et al*. Cancer immunotherapy with recombinant poliovirus induces IFN-dominant activation of dendritic cells and tumor antigen-specific CTLs. *Sci Transl Med* 2017;9:eaan4220.

14 Holl EK, Brown MC, Boczkowski D, *et al*. Recombinant oncolytic poliovirus, PVSRIPO, has potent cytotoxic and innate inflammatory effects, mediating therapy in human breast and prostate cancer xenograft models. *Oncotarget* 2016;7:79828–41.

15 Yang Y, Brown MC, Zhang G, *et al*. Polio virotherapy targets the malignant glioma myeloid infiltrate with diffuse microglia activation engulfing the CNS. *Neuro Oncol* 2023:noad052.

16 Brown MC, Bryant JD, Dobrikova EY, *et al*. Induction of viral, 7-methyl-guanosine cap-independent translation and oncolysis by mitogen-activated protein kinase-interacting kinase-mediated effects on the serine/arginine-rich protein kinase. *J Virol* 2014;88:13135–48.

17 Hawken J, Troy SB. Adjuvants and inactivated polio vaccine: a systematic review. *Vaccine* 2012;30:6971–9.

18 Swain SL. Generation and in vivo persistence of polarized th1 and th2 memory cells. *Immunity* 1994;1:543–52.

19 Mosaheb MM *et al*. Genetically stable poliovirus vectors activate dendritic cells and prime antitumor CD8 T cell immunity. *Nat Commun* 2020;11:524.

20 Blanchard C, Rothenberg ME. Biology of the eosinophil. *Adv Immunol* 2009;101:81–121.

21 Mittrücker HW, Matsuyama T, Grossman A, *et al*. Requirement for the transcription factor lsirf/irf4 for mature b and t lymphocyte function. *Science* 1997;275:540–3.

22 Groeneveldt C, Kinderman P, van Stigt Thans JJC, *et al*. Preinduced reovirus-specific t-cell immunity enhances the anticancer efficacy of reovirus therapy. *J Immunother Cancer* 2022;10:e004464.

23 Selvanesan BC *et al*. Listeria delivers tetanus toxoid protein to pancreatic tumors and induces cancer cell death in mice. *Sci Transl Med* 2022;14:eabc1600.

24 Tähtinen S, Feola S, Capasso C, *et al*. Exploiting preexisting immunity to enhance oncolytic cancer immunotherapy. *Cancer Res* 2020;80:2575–85.

25 Cachot A, Bilous M, Liu Y-C, *et al*. Tumor-specific cytolytic cd4 t cells mediate immunity against human cancer. *Sci Adv* 2021;7:eabe3348.

26 Oh DY, Kwek SS, Raju SS, *et al*. Intratumoral cd4+ t cells mediate anti-tumor cytotoxicity in human bladder cancer. *Cell* 2020;181:1612–25.

27 Quezada SA, Simpson TR, Peggs KS, *et al*. Tumor-reactive CD4 (+) T cells develop cytotoxic activity and eradicate large established melanoma after transfer into lymphopenic hosts. *J Exp Med* 2010;207:637–50.

28 Perez-Diez A, Joncker NT, Choi K, *et al*. Cd4 cells can be more efficient at tumor rejection than CD8 cells. *Blood* 2007;109:5346–54.

29 Corthay A, Skovseth DK, Lundin KU, *et al*. Primary antitumor immune response mediated by CD4+ T cells. *Immunity* 2005;22:371–83.

30 Church SE, Jensen SM, Antony PA, *et al*. Tumor-Specific CD4+ T cells maintain effector and memory tumor-specific CD8+ T cells. *Eur J Immunol* 2014;44:69–79.

31 Lu Z, Yuan L, Zhou X, *et al*. Cd40-Independent pathways of T cell help for priming of CD8 (+) cytotoxic T lymphocytes. *J Exp Med* 2000;191:541–50.

32 Hung K, Hayashi R, Lafond-Walker A, *et al*. The central role of CD4 (+) T cells in the antitumor immune response. *J Exp Med* 1998;188:2357–68.

33 Simon SCS, Hu X, Panten J, *et al*. Eosinophil accumulation predicts response to melanoma treatment with immune checkpoint inhibitors. *Oncoimmunology* 2020;9:1727116.

34 Mackensen A, Meidenbauer N, Vogl S, *et al*. Phase I study of adoptive T-cell therapy using antigen-specific CD8+ T cells for the treatment of patients with metastatic melanoma. *J Clin Oncol* 2006;24:5060–9.

35 Jacquelot N, Seillet C, Wang M, *et al*. Blockade of the co-inhibitory molecule PD-1 unleashes ILC2-dependent antitumor immunity in melanoma. *Nat Immunol* 2021;22:851–64.

36 Blomberg OS, Spagnuolo L, Garner H, *et al*. IL-5-producing cd4+ t cells and eosinophils cooperate to enhance response to immune checkpoint blockade in breast cancer. *Cancer Cell* 2023;41:106–23.

37 Thorsson V, Gibbs DL, Brown SD, *et al*. The immune landscape of cancer. *Immunity* 2018;48:812–30.

38 Newman AM, Steen CB, Liu CL, *et al*. Determining cell type abundance and expression from bulk tissues with digital cytometry. *Nat Biotechnol* 2019;37:773–82.

39 Lloyd CM, Snelgrove RJ. Type 2 immunity: expanding our view. *Sci Immunol* 2018;3:eaat1604.

40 Oliphant CJ, Hwang YY, Walker JA, *et al*. MHCII-mediated dialog between group 2 innate lymphoid cells and cd4(+) t cells potentiates type 2 immunity and promotes parasitic helminth expulsion. *Immunity* 2014;41:283–95.

41 Moynihan KD, Opel CF, Szeto GL, *et al*. Eradication of large established tumors in mice by combination immunotherapy that engages innate and adaptive immune responses. *Nat Med* 2016;22:1402–10.

42 Kouro T, Takatsu K. IL-5- and eosinophil-mediated inflammation: from discovery to therapy. *Int Immunol* 2009;21:1303–9.

43 Barthel FP, Johnson KC, Varn FS, *et al*. Longitudinal molecular trajectories of diffuse glioma in adults. *Nature* 2019;576:112–20.

44 Alspach E, Lussier DM, Miceli AP, *et al*. MHC-II neoantigens shape tumour immunity and response to immunotherapy. *Nature* 2019;574:696–701.

45 Laidlaw BJ, Craft JE, Kaech SM. The multifaceted role of CD4 (+) T cells in CD8 (+) T cell memory. *Nat Rev Immunol* 2016;16:102–11.

46 Arnold IC, Artola-Boran M, Gurtner A, *et al*. The GM-CSF-IRF5 signaling axis in eosinophils promotes antitumor immunity through activation of type 1 T cell responses. *J Exp Med* 2020;217:e20190706.

47 Bachmann MF, Rohrer UH, Kündig TM, *et al*. The influence of antigen organization on B cell responsiveness. *Science* 1993;262:1448–51.

48 Link A, Zabel F, Schnetzler Y, *et al*. Innate immunity mediates follicular transport of particulate but not soluble protein antigen. *J Immunol* 2012;188:3724–33.

49 Trabanelli S, Chevalier MF, Derré L, *et al*. The pro- and anti-tumor role of ilc2s. *Semin Immunol* 2019;41:101276.

50 Simon SCS, Utikal J, Umansky V. Opposing roles of eosinophils in cancer. *Cancer Immunol Immunother* 2019;68:823–33.

51 Lloyd CM, Hessel EM. Functions of T cells in asthma: more than just T (H) 2 cells. *Nat Rev Immunol* 2010;10:838–48.

52 Smith SG, Chen R, Kjarsgaard M, *et al*. Increased numbers of activated group 2 innate lymphoid cells in the airways of patients with severe asthma and persistent airway eosinophilia. *J Allergy Clin Immunol* 2016;137:75–86.

53 Moral JA, Leung J, Rojas LA, *et al*. Ilc2S amplify PD-1 blockade by activating tissue-specific cancer immunity. *Nature* 2020;579:130–5.

54 Huang Z, Wu L, Hou Z, *et al*. Eosinophils and other peripheral blood biomarkers in glioma grading: a preliminary study. *BMC Neurol* 2019;19:313.

55 Ostrom QT, Lu D, Lu R, *et al*. Prevalence of autoimmunity and atopy in US adults with glioblastoma and meningioma. *Neuro Oncol* 2022;24:1807–9.

56 Tuzlak S, Dejean AS, Iannacone M, *et al*. Repositioning th cell polarization from single cytokines to complex help. *Nat Immunol* 2021;22:1210–7.

57 Nishimura T, Iwakabe K, Sekimoto M, *et al*. Distinct role of antigen-specific T helper type 1 (Th1) and Th2 cells in tumor eradication in vivo. *J Exp Med* 1999;190:617–27.

58 Lorvik KB, Hammarström C, Fauskanger M, *et al*. Adoptive transfer of tumor-specific Th2 cells eradicates tumors by triggering an in situ inflammatory immune response. *Cancer Res* 2016;76:6864–76.

59 Vonderheide RH. Cd40 agonist antibodies in cancer immunotherapy. *Annu Rev Med* 2020;71:47–58.

60 Ott PA, Hu Z, Keskin DB, *et al*. An immunogenic personal neoantigen vaccine for patients with melanoma. *Nature* 2017;547:217–21.

SUPPLEMENTARY INFORMATION

Intratumoral Childhood Vaccine-Specific CD4$^+$ T cell Recall
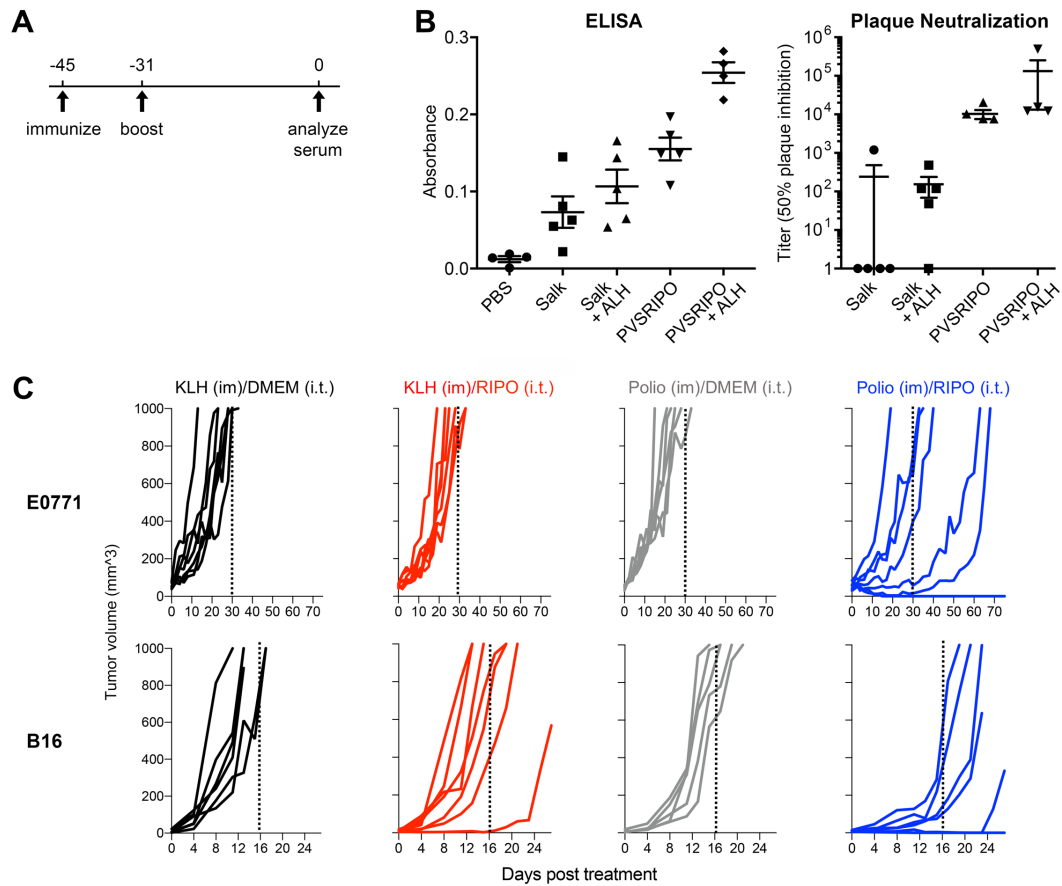
Coordinates Antitumor CD8$^+$ T cells and Eosinophils

Brown, MC et al., 2023

This file contains:
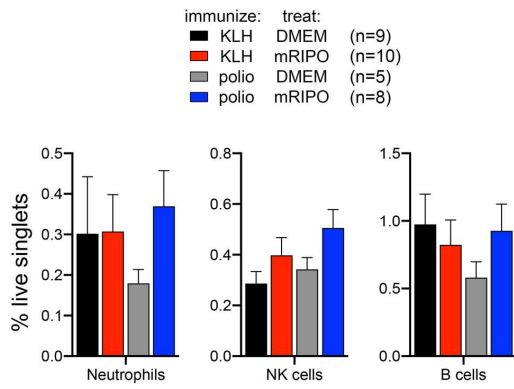**Supplementary Figures 1-13**
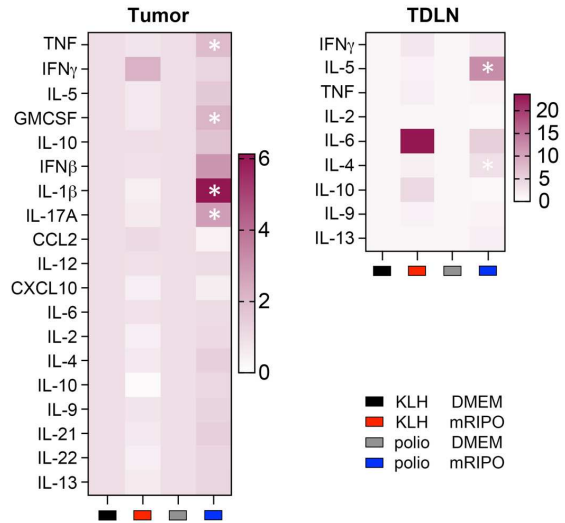**Supplementary Table 1**
Supplementary methods

Supplementary Figure 1. (**A**) Schema for immunization validation in (**B**). (**B**) ELISA (left) and plaque neutralization assay (right) from serum of mice immunized as shown (n= 5/group). (**C**) Individual tumor volumes from experiments shown in Figure 1B.
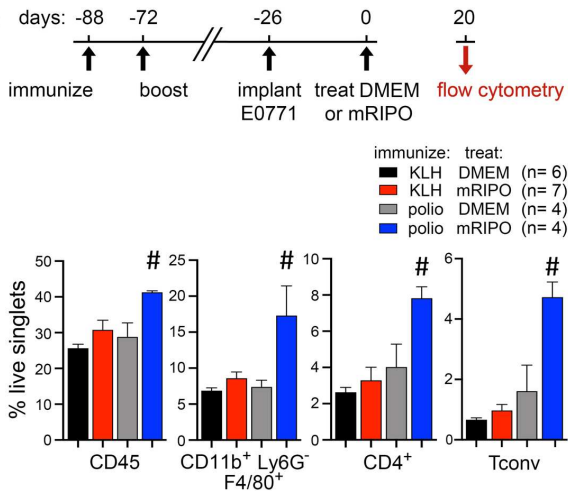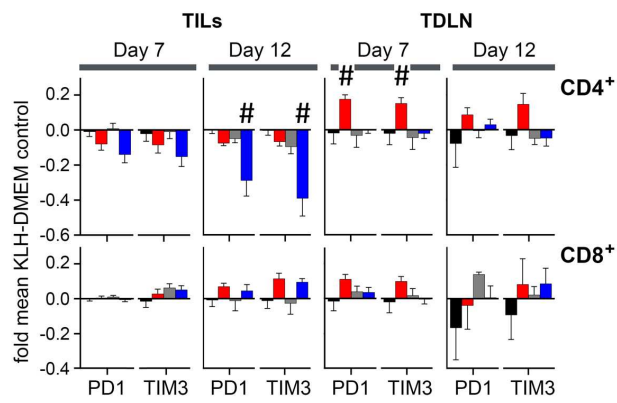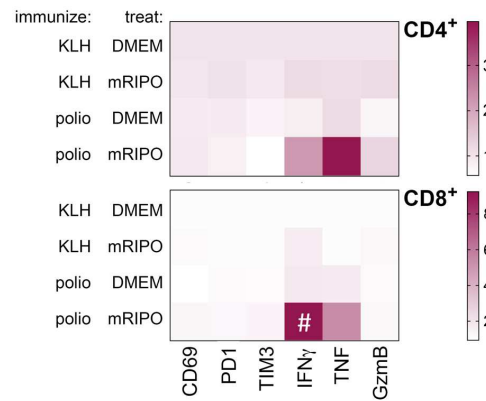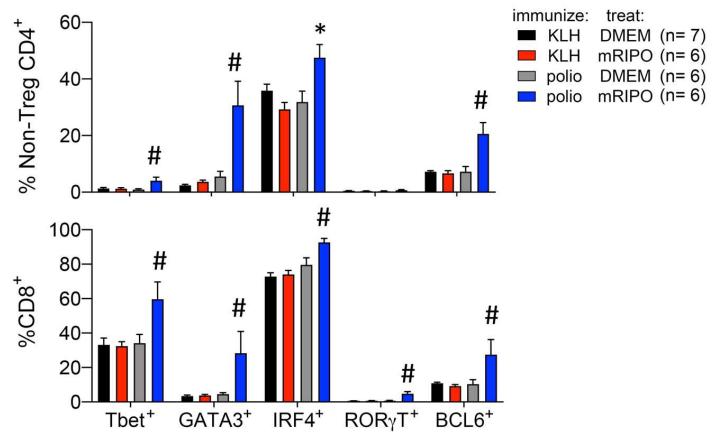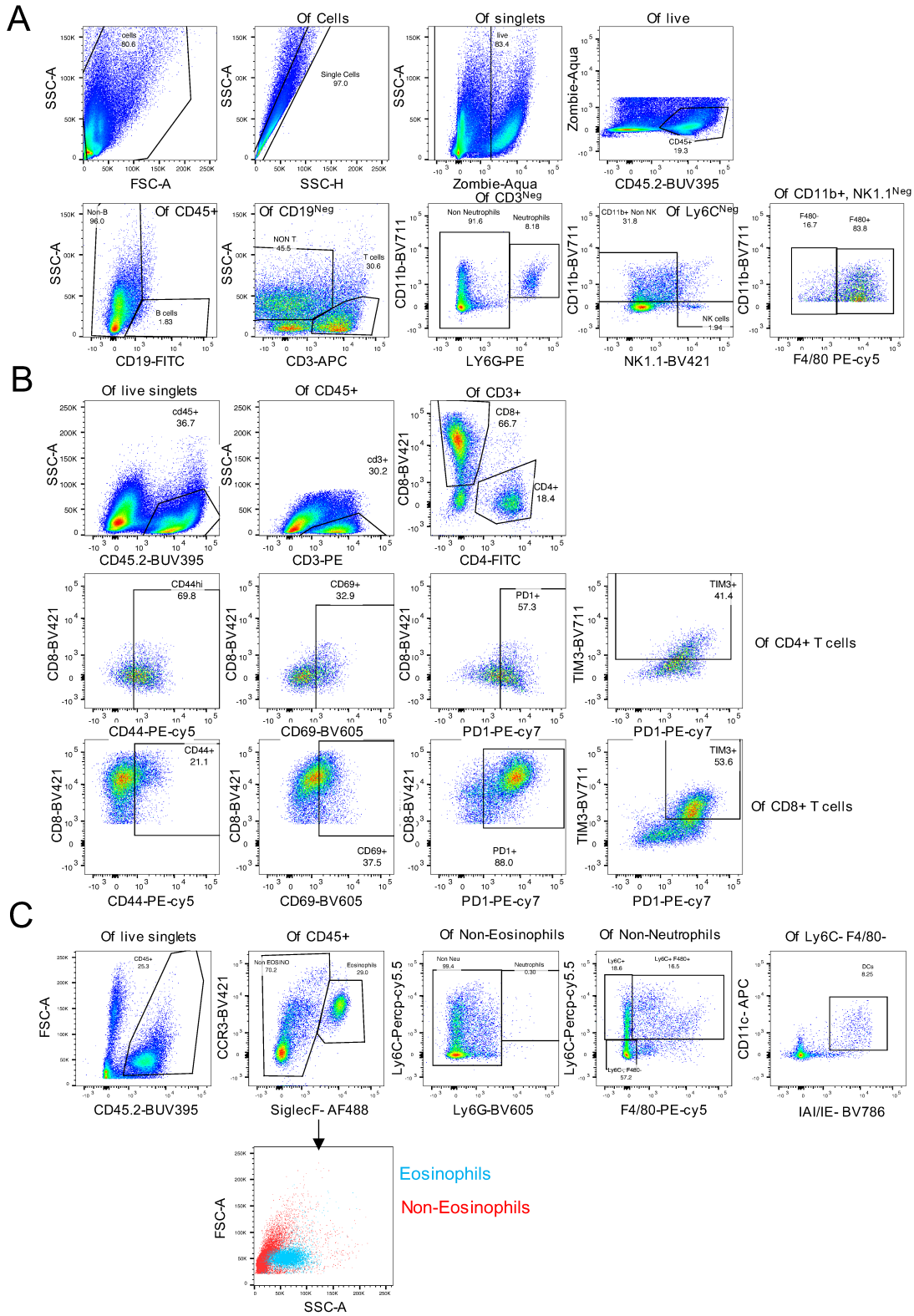
Supplementary Figure 2. (**A**) Density of neutrophils, NK cells, and B cells from the experiment presented in Figure 1E. (**B**) (Left) B16 tumor homogenate cytokines 7 days after intratumor mock (DMEM) or mRIPO treatment in KLH or polio immunized mice were measured and normalized to fold respective mean mock control values; asterisks indicate Tukey's post hoc test $p<0.05$ versus mock controls (n=5/group KLH immunized; n=8/group polio immunized). (Right) TDLN cells from KLH or polio immunized B16 tumor bearing mice 7 days after treatment with DMEM or mRIPO were cultured in RPMI 1640+10% FBS for 24 hours and cytokine release was measured (n=2 KLH-DMEM, n=4 for all others); asterisks indicate Kruskal-Wallis post-hoc test $p<0.05$. (**C**) Experimental schema and analyses of infiltrating immune cells in the E0771 model, as done in Figure 1E for the B16 model. (**D**) PD1 and TIM3 surface staining on CD4+ and CD8+ T cells from tumor (TILs) or tumor draining lymph node (TDLN) derived single cell suspensions using the same samples analyzed in Figure 1G-F at day 12 post treatment, values were normalized to log(fold mean KLH-DMEM control). (**E, F**) Analysis of TIL phenotypes in the E0771 model for experiment presented in (C), as done for the B16 model in Fig 1G-F. (**A, C, D, F**) Data bars represent mean + SEM; (**E**) values were normalized as fold mean KLH-DMEM for each marker; (**C-F**) asterisks denote Dunnett's multiple comparison test vs corresponding DMEM treated controls ($p<0.05$, two tailed); # indicates significant Tukey's post-hoc test vs all other groups.

BMJ Publishing Group Limited (BMJ) disclaims all liability and responsibility arising from any reliance placed on this supplemental material which has been supplied by the author(s)

Supplemental material

J Immunother Cancer

Supplemental material

BMJ Publishing Group Limited (BMJ) disclaims all liability and responsibility arising from any reliance placed on this supplemental material which has been supplied by the author(s)

J Immunother Cancer

Supplementary Figure 3. Representative gating strategy for tumor infiltrating cells analyzed in Figures 1E-F and S2. Live singlets were selected after gating of cells, followed by single cells via forward scatter (FSC-A) vs height (FSC-H) comparison, and live/dead using Zombie-Aqua as shown. (**A**) Myeloid cell panel used to gate for B cells, T cells, myeloid cells, and NK cells as shown. (**B**) T cell panel used to gate for CD4$^+$ and CD8$^+$ T cells as well as gating for the indicated antigens on each. (**C**) Eosinophil and myeloid panel to determine the identity of CD11b+ F4/80+ cells identified in Figure 1E: CCR3 and Siglec F were used to gate for eosinophils relative to other myeloid populations and DCs. Confirmation of eosinophil identity was corroborated via confirming their granulocyte identity via SSC-A, and confirming they were Ly6C$^{low/neg}$.

BMJ Publishing Group Limited (BMJ) disclaims all liability and responsibility arising from any reliance placed on this supplemental material which has been supplied by the author(s)

Supplemental material

J Immunother Cancer
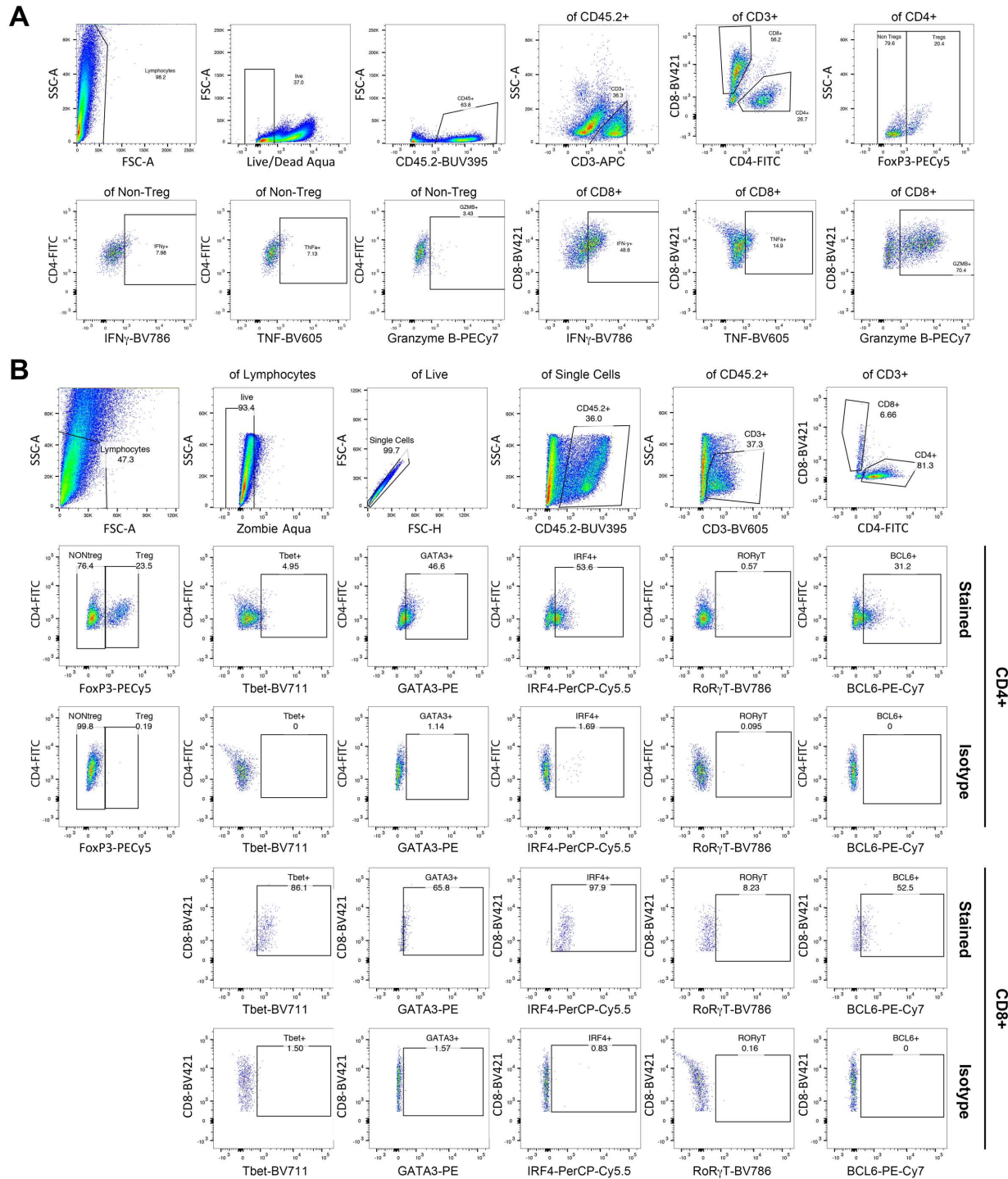
Supplementary Figure 4. Representative gating strategy for TIL activation/differentiation status as shown in Figures 1H and S2. Live/dead and singlet discrimination was performed as described in Figure S3. (**A**) T cell panel to determine conventional CD4$^+$ T cell, Treg, and CD8$^+$ densities as well as expression of the indicated intracellular cytokines and granzyme B as shown in Figure 1E and G. (**B**) T cell panel to measure T cell associated transcription factors as shown in Figure 1H; isotype controls for transcription factors were used as shown to guide gating.
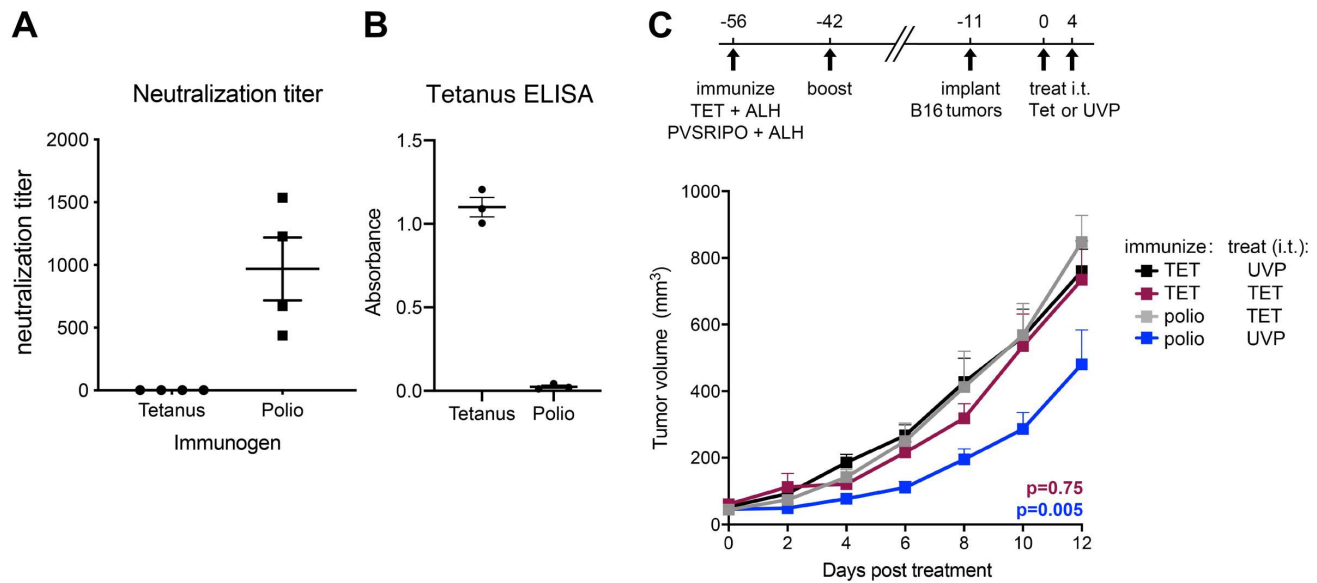
Supplementary Figure 5. (**A, B**) Validation of immunogen-specific serum antibodies for immunization strategies in Figure 2A and B by PVSRIPO plaque neutralization assay (**A**; n= 4/group) and tetanus ELISA (**B**; n= 3/group); mean -/+ SEM is shown. (**C**) Repeat tumor therapy experiment for Figure 2A. Mean tumor volume + SEM are shown (Polio-Tet and Tet-UVP: n= 7; Tet-Tet: n= 6; Polio-UVP: n= 8).

Supplemental material

BMJ Publishing Group Limited (BMJ) disclaims all liability and responsibility arising from any reliance placed on this supplemental material which has been supplied by the author(s)

J Immunother Cancer
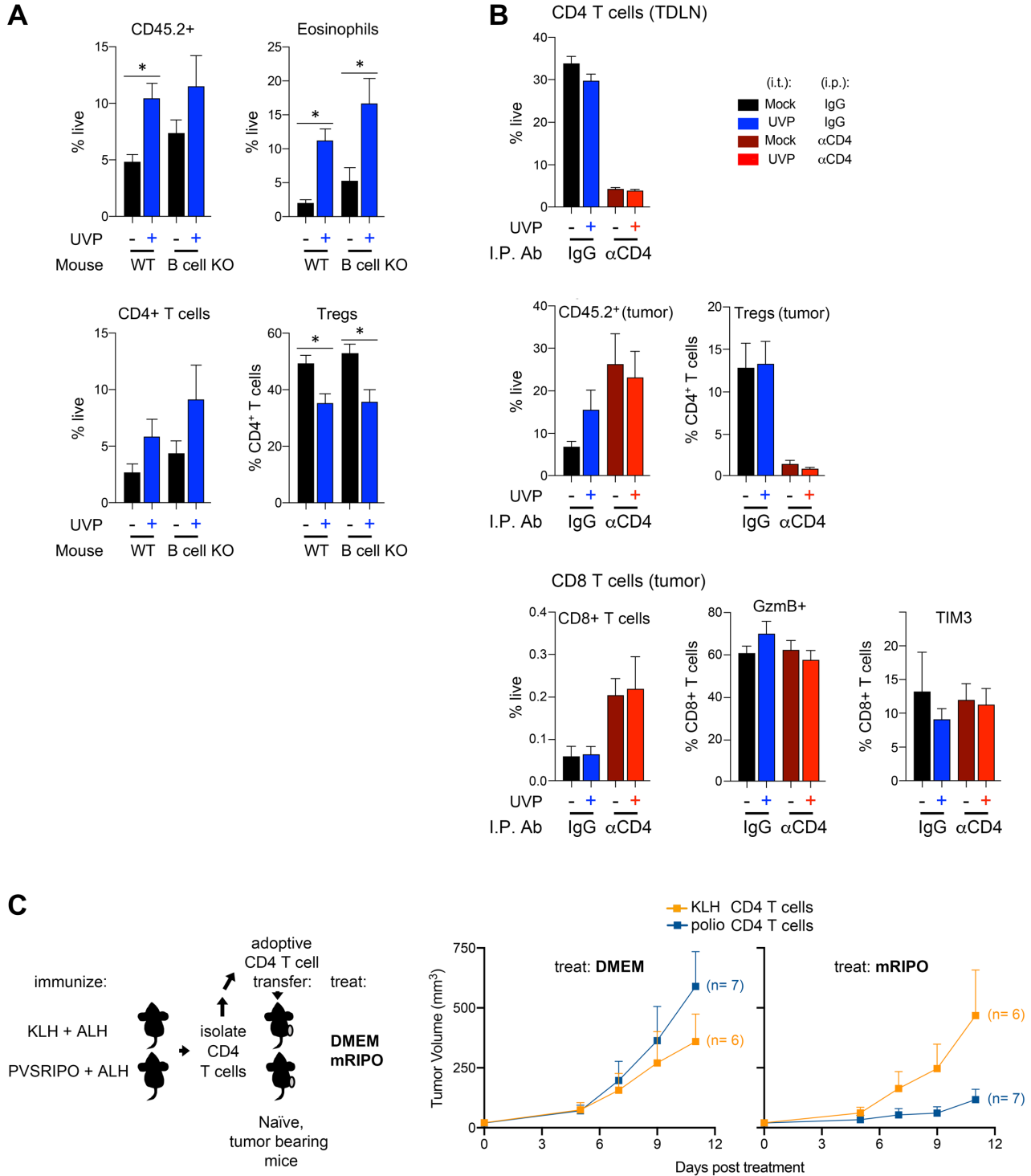
Supplementary Figure 6. Extended analyses from experiments in Figure 3. (**A**) Flow cytometry analysis of tumors 12 days after mock or UVP from wt or B cell k/o mice immunized and treated as in Figure 3A; mean + SEM is shown; (*) Tukey's post hoc test $p < 0.05$. (**B**) Extended flow cytometry analysis of tumors and TDLN from Figure 3D; mean + SEM is shown. (**C**) Tumor volumes from repeat experiment of the assay described in Figure 3E, using CD4$^+$ T cells from KLH or polio immunized mice. Mean tumor volume + SEM are shown.
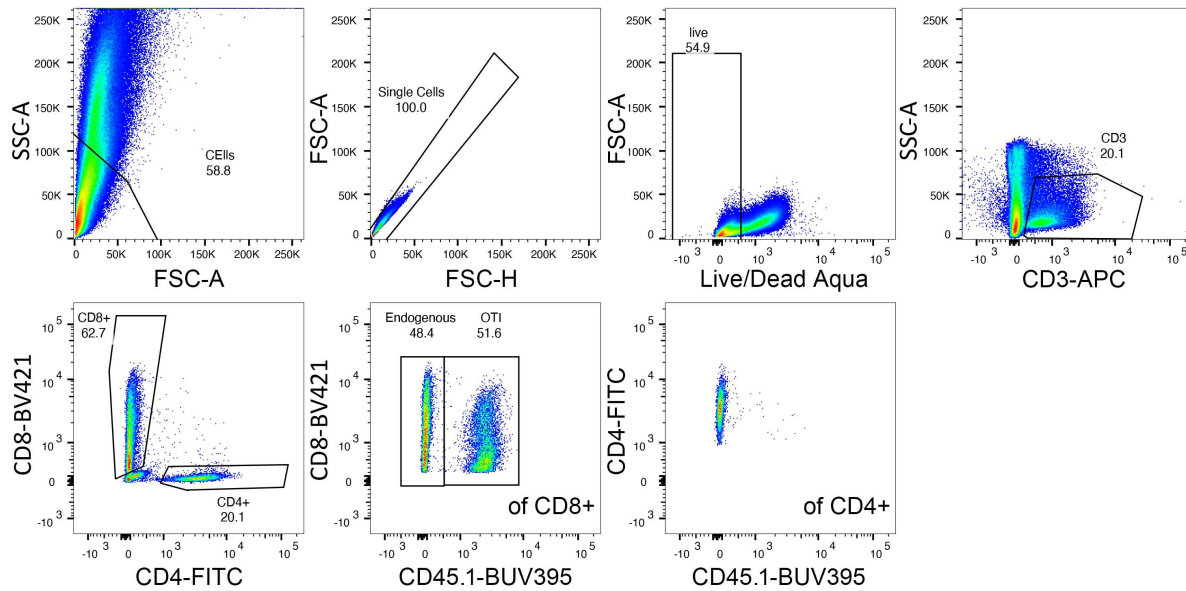
Supplementary Figure 7. Gating strategy for OT-I (CD45.1$^+$) vs endogenous (CD45.1^{Neg}) CD8$^+$ T cells in tumors from experiments presented in Figures 4 and S10; gating for markers of activation and differentiation were conducted as shown in Figure S4.
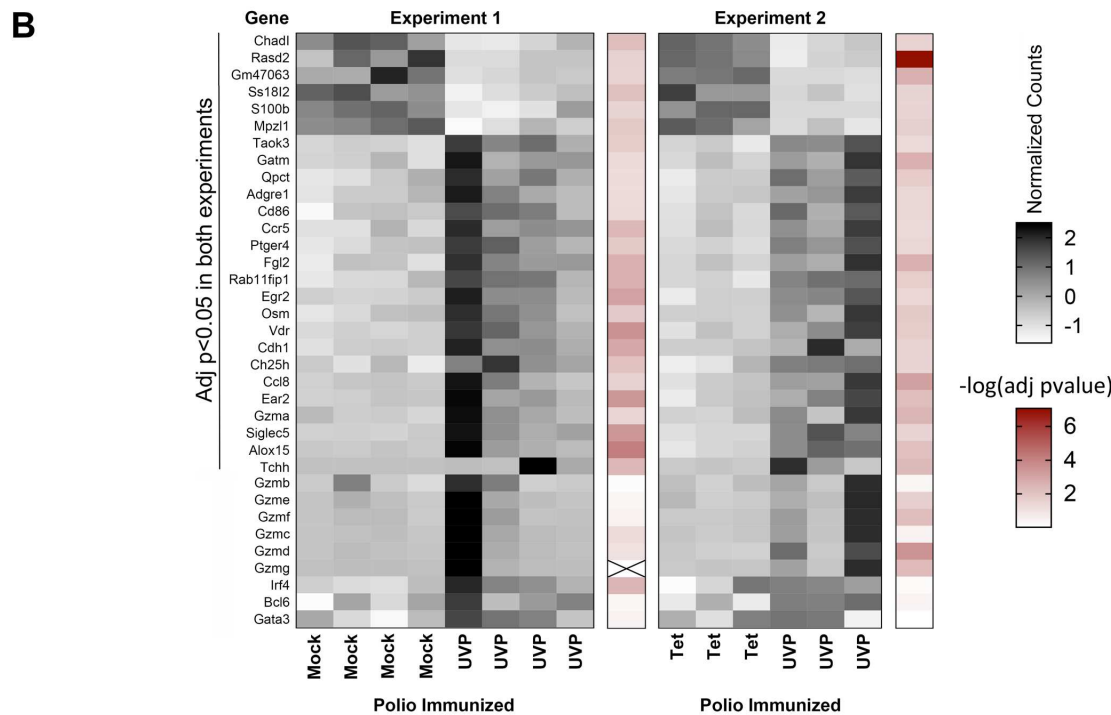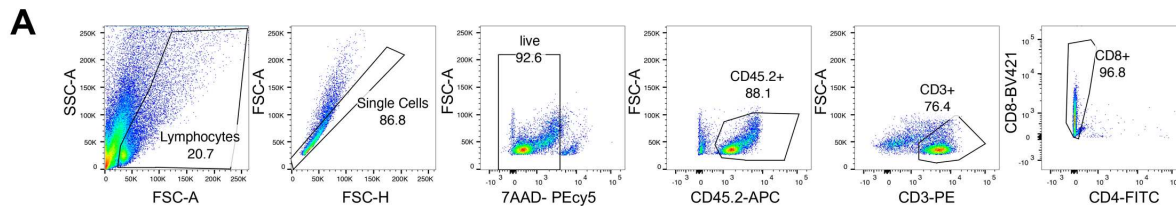
C

| Gene name(s)	After UVP	Full name	Relevance	Ref
Chadl	Down	Chondroadherein like	Collogen binding	Uniprot
S100b	Down	S100 calcium binding protein B	expressed in subsets of CTLs, RAGE and NFkb signaling	PMIDs: 19121341, 11705636, 21447379
Gm47063	Down	predicted gene, 47063	Unknown	Uniprot
Rasd2, Viperin	Down	Radical S-Adenyosyl Methionine Domain Containing 2	IFN inducible; Th2 polarization, TCR activation of NFkB and AP-1	PMID: 19047684
Ss18l2	Down	SS18-like protein 2	Unknown	Uniprot
Mpzl1	Down	Myelin Protein Zero Like 1	SRC/SHP2 signaling: SHP2 signaling may suppress antitumor T cell function	PMIDs: 24296779, 33446805, 19290938
Taok3	Up	TAO kinase 3	T cell activation, prevents SHP1 mediated inactivation	PMID: 30373850
Rab11fip1	Up	RAB11 Family Interaacting Protein 1	endosomal recycling, intracellular transport; associated with immune cell influx in cancer	Uniprot; PMID 34764984
Ptger4	Up	Prostaglandin E receptor 4	promotes Th1 differentiation; upregulated on Th17 T cells	PMIDs: 23575689, 29935220
CD86; B7	Up	CD86 molecule	expressed on APCs, Expressed by effector memory T cells	Uniprot; PMID: 9973476
Ccr5	Up	CC motif chemokine receptor 5	chemokine receptor; expressed by activated T cells	PMID: 18632580
Ch25h	Up	cholesterol 25-hydrocylase	produces 25HC; inflammation during viral infection; constrains T cell inflammation in skin	PMIDs: 24994901, 34623903
Osm	Up	oncostatin M	IL6 family, released by T cells, promotes activation of SOCS3, STAT3, STAT5	PMIDs: 17372020, 28093521
Egr2	Up	Early growth response 2	Induce SOCS1/SOCS3 signaling; supports T cell proliferation and homeostasis	PMIDs: 23021953, 25368162
Adgre1; F4/80	Up	Adhesion G Protein-Coupled Receptor E1	cell adhesion, expressed on antiviral CD8 T cells	PMID: 14515257
Vdr	Up	Vitamin D Receptor	T cell development, differentiation, and effector function	PMID: 23785369
Qpct	Up	glutaminyl-peptide cyclotransferase	conversion of N-terminal glutamic acid into pyroglutamine	PMID: 23183267
Fgl2	Up	Fibrinogen-like protein 2	Expressed by CTLs, type I immunity, IRF1 dependent	PMIDs: 3550794, 14976252
Gatm	Up	Glycine amidinotransferase	creatinine biosythesis	Uniprot
Ear2	Up	Eosinophil-associated, ribonuclease A family member 2	eosinophils; cytotoxicity	Uniprot
Alox15	Up	Arachidonate 15-Lipoxygenase	induced by Th2 responses; Fatty acid oxidation; Treg homeostasis	Uniprot, PMIDs: 31333453, 34040168
Siglec5	Up	Sialic acid-binding Ig-like lectin 5	expressed by eosinophils, induced on activated CD8 T cells	Uniprot, PMID: 17272508
Ccl8; MCP2	Up	C-C motif chemokine ligand 8	Skin accumulation of Th2 cells	PMID: 21245898
Gzma	Up	Granzyme A	Cytolysis	Uniprot
Cdh1	Up	cadherin 1	adherence	Uniprot
Tchh	Up	trichohylin	Unknown	Uniprot
Gzmb	Up	Granzyme B	Cytolysis	Uniprot
Gzme	Up	Granzyme E	Cytolysis	Uniprot
Gzmf	Up	Granzyme F	Cytolysis	Uniprot
Gzmc	Up	Granzyme C	Cytolysis	Uniprot
Gzmd	Up	Granzyme D	Cytolysis	Uniprot
Gzmg	Up	Granzyme G	Cytolysis	Uniprot
Irf4	Up	Interferon regulatory factor 4	CD8 T cell effector memory function	Uniprot; PMIDs: 33859042; 24835398
Bcl6	Up	B-cell lymphoma 6	Controls Granzyme expression in CD8 T cells	Uniprot; PMID 17125145
Gata3	Up	GATA Binding Protein 3	type 2 cytokines by CD8 T cells, CD8 T cell homeostasis	Uniprot; PMID 23225883

Supplementary Figure 8. (**A**) Validation of CD45.1+ OT-I+ enrichment after positive CD45.1 selection using tumor suspensions in experiments in Fig 4C; note that OT-I T cells are positive for both CD45.2 and CD45.1, while endogenous T cells were only CD45.2+. (**B**) Normalized transcript counts (black) and -log(False Discovery Rate adjusted p-value) (red) for genes significantly different between OT-I T cells after polio recall (polio immunized mice treated with UVP) vs Mock or Tet treatment in polio immunized mice in two independent experiments as indicated by annotation in figure. In addition, relevant transcripts with protein changes in flow cytometry analyses (Fig 4C): granzymes, IRF4, BCL6, and GATA3 that approached significance in both studies were included; a p-value for Gzmg was not assigned in experiment 1 due to an outlier. (**C**) Table presents known relevance of genes from (B) to T cell biology (PMID= Pub Med ID) and directionality for change (consistent in both replicates) after treatment with UVP in polio immunized mice from two independent experiments.
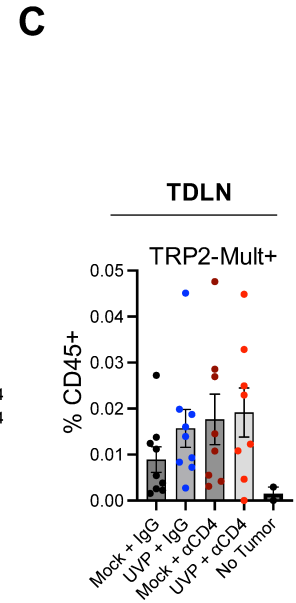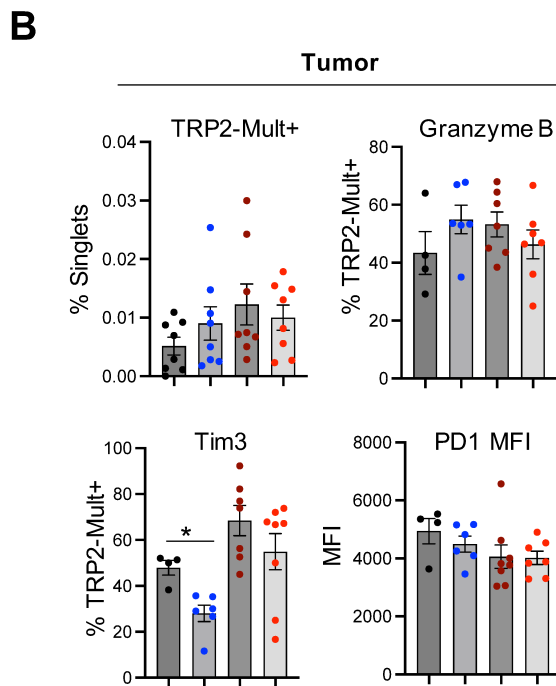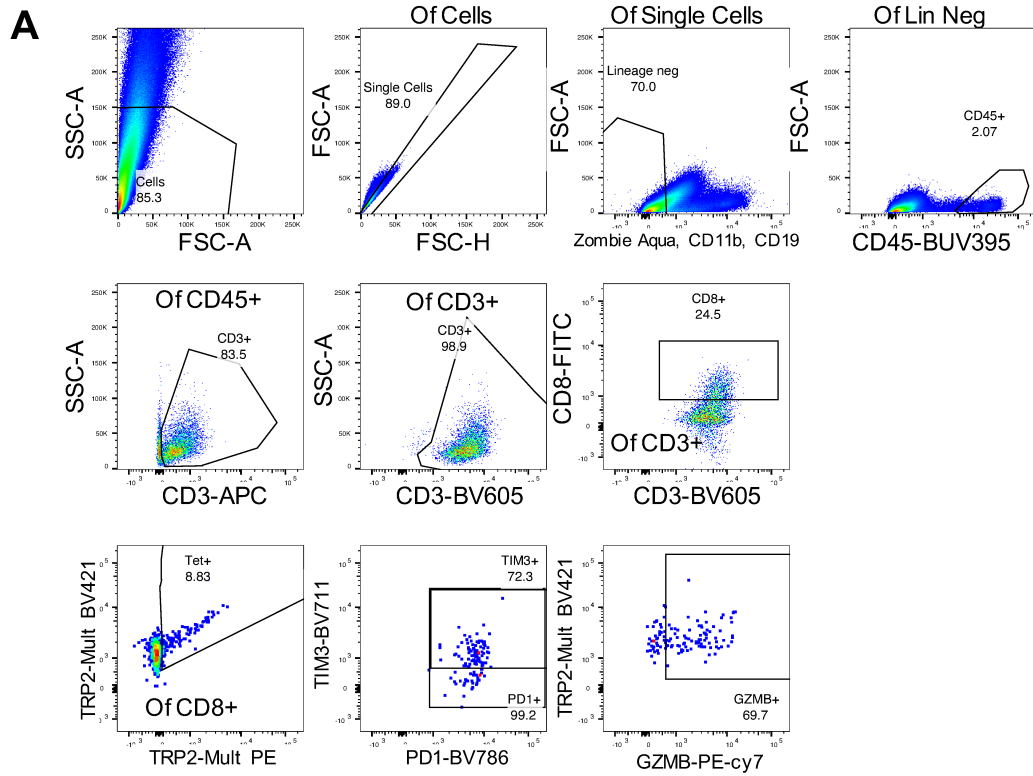
Supplementary Figure 9. TRP2-MHC class I multimer (TRP2-Mult)-specific T cells after polio recall with and without CD4$^+$ T cell depletion. (**A**) Gating strategy for TRP2-MHC-class I multimer (TRP2-Mult) specific TILs in B16 tumors. (**B, C**) Density and phenotype of TRP2-multimer specific CD8$^+$ TILs (B), or percentage of TRP2-multimer specific CD8$^+$ T cells out of CD45+ cells from the TDLN (C). Lymph nodes from non-tumor bearing mice ("No Tumor") were used to confirm specificity of multimer staining. Each data point indicates individual mice; bars and brackets indicate mean -/+ SEM. For phenotypes of TRP2+ T cells, samples with less than 20 TRP2-Multimer+ events were excluded. Note that CD4$^+$ T cell depletion primarily depleted Tregs, which may explain increased levels of TRP2-multimer specific CD8$^+$ T cells in tumors and TDLNs after CD4 T cell depletion (Fig S6).
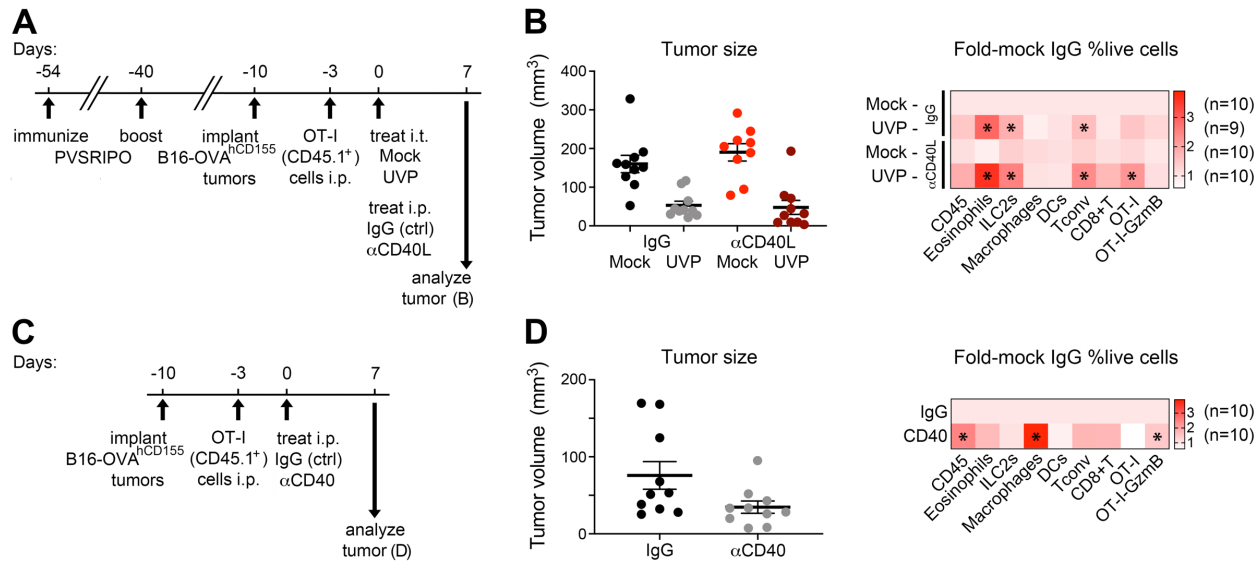
Supplementary Figure 10. The antitumor efficacy of recall antigens is independent of CD40L-CD40 signaling. (**A**) B16-OVA tumor bearing mice previously immunized against polio received adoptive transfer of OT-I T cells followed by intratumor treatment with either mock or UVP concomitant with control IgG or a CD40L blocking antibody (250µg, every 3 days) for experiment shown in (**B**). (**B**) Tumor volume (left) and analysis of tumor infiltrating immune cells (right) was conducted 7 days after treatment. Data bars depict mean -/+ SEM; heatmap depicts fold-mock IgG control. (**C**) B16-OVA tumor bearing mice received adoptive transfer of OT-I cells followed by intraperitoneal treatment with control IgG or anti-CD40 antibody (50µg/mouse, once) for experiment shown in (**D**). (**D**) Tumor volume (left) and analysis of tumor infiltrating immune cells (right) were measured 7 days after treatment. Data bars depict mean -/+ SEM; heatmap depicts fold-mock IgG control. Asterisks indicate Dunnett's post-hoc test relative to mock + IgG control (**B**), or unpaired t test relative to IgG control (**D**). All experiments were repeated at least twice and representative series are shown.

Supplemental material

BMJ Publishing Group Limited (BMJ) disclaims all liability and responsibility arising from any reliance placed on this supplemental material which has been supplied by the author(s)

J Immunother Cancer
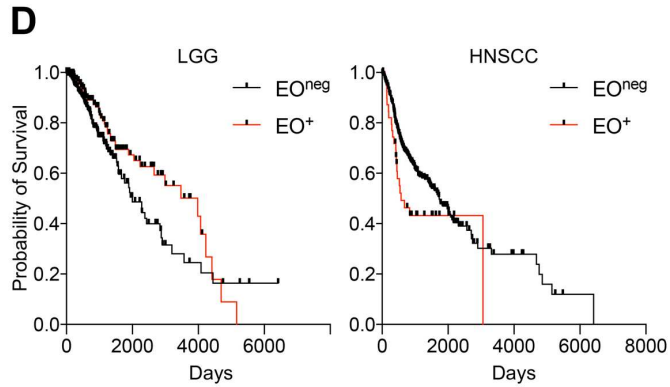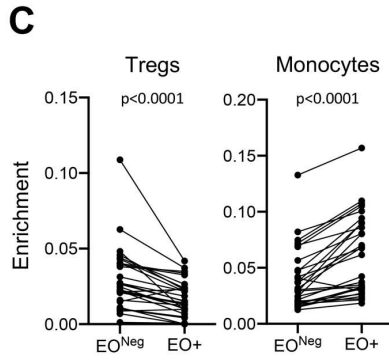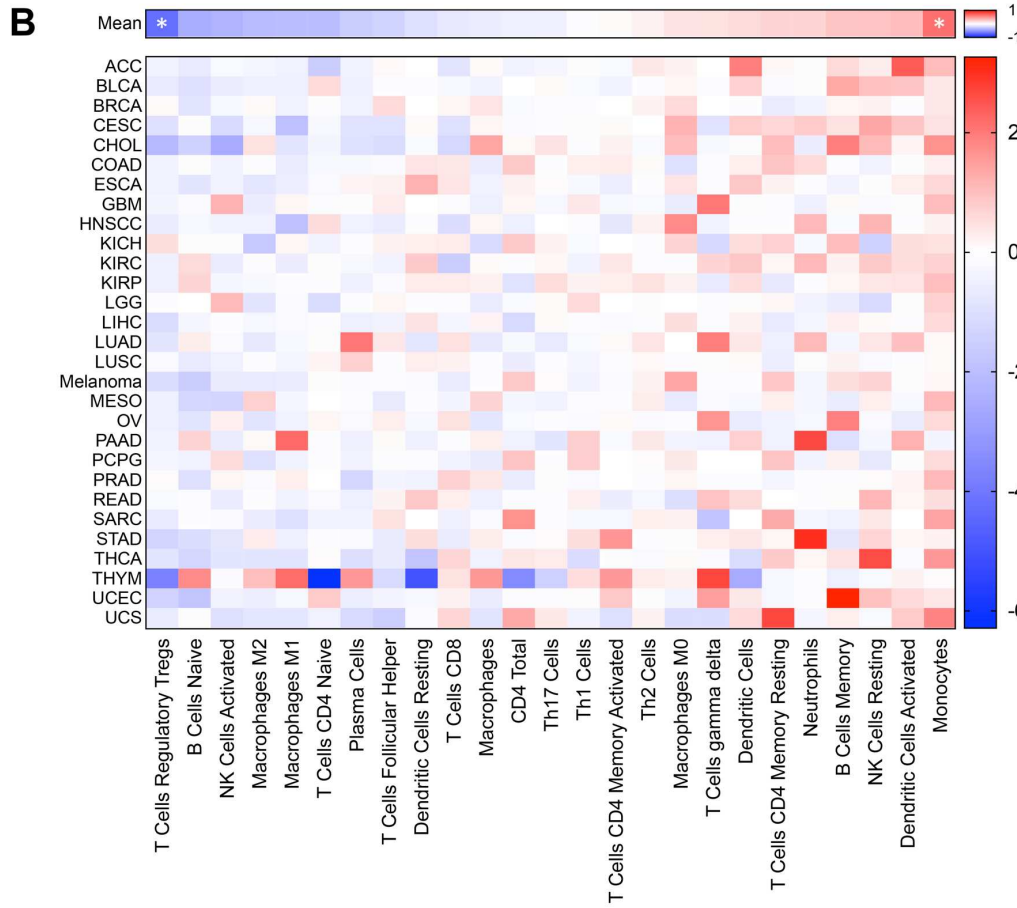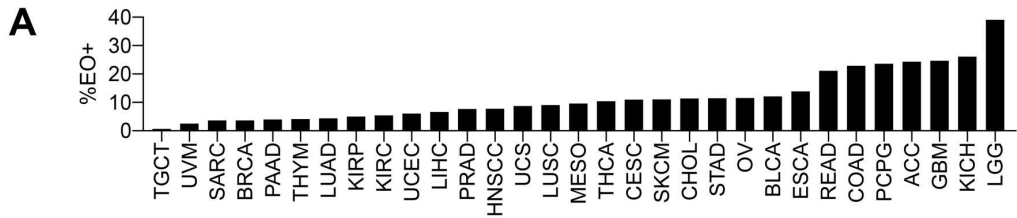
Supplementary Figure 11. Pan-cancer analysis of frequency of eosinophil detection by CIBERSORT within each cancer type (**A**); changes in the frequency of cell types associated with the presence vs absence of detected eosinophils (**B, C**); and survival of LGG and HNSCC by eosinophil detection vs absence corresponding to Figure 5A-B (**D**). (**B**) Asterisks denote significant False Discovery Rate adjusted paired t-test comparing cell type densities across cancer types (n=29); (**C**) p-values are from paired t-test for monocytes and Tregs across cancer types (n=29); (**B, C**) each cancer type was treated as one pair.
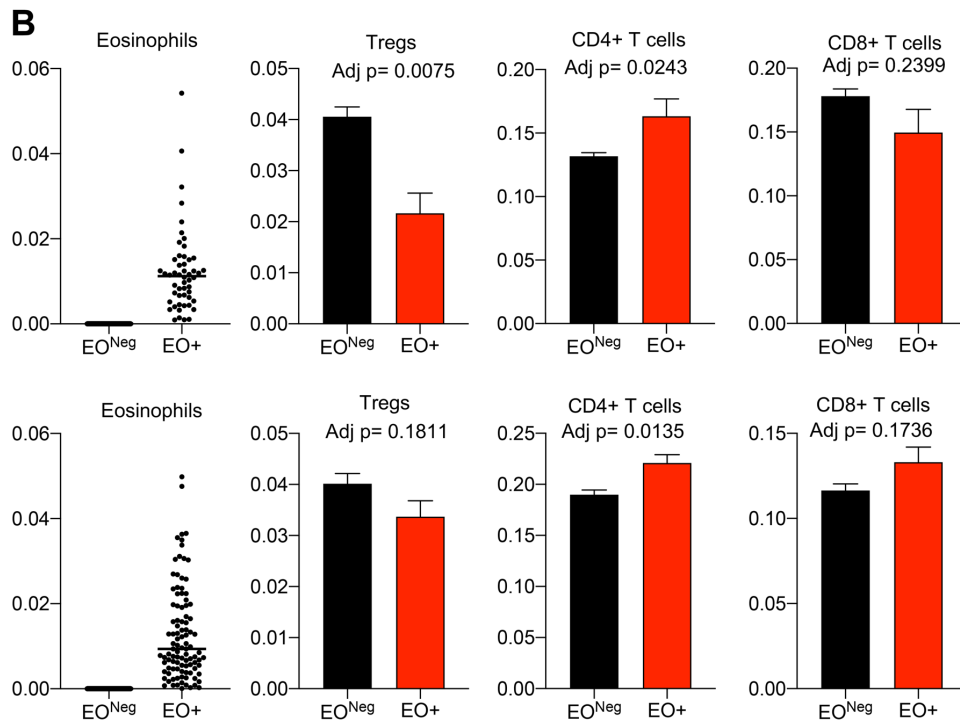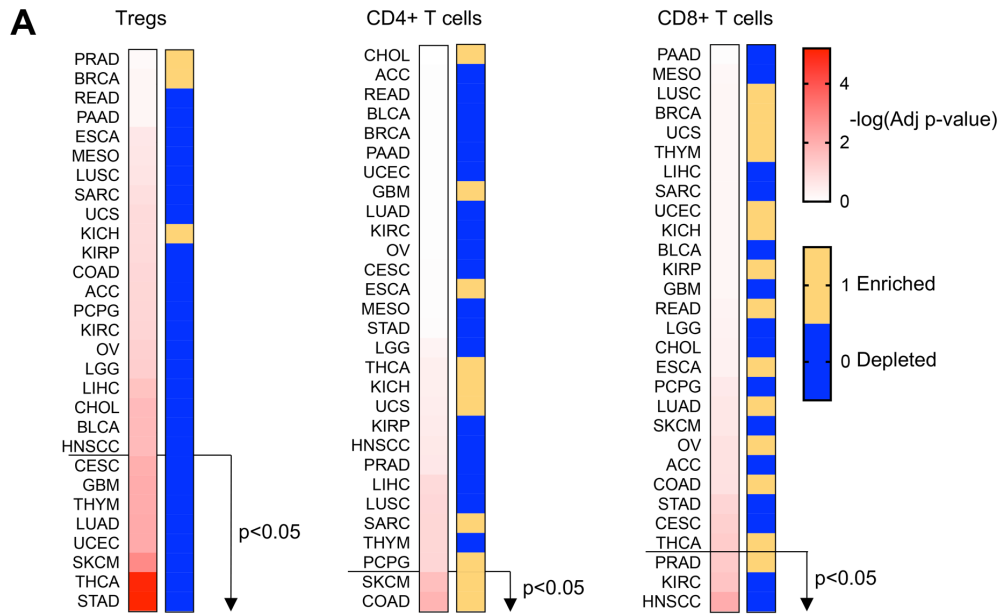
Supplementary Figure 12. (**A**) Pan-cancer analysis conducted in Fig 5A and Supplementary Figure 11, presenting False Discovery Rate corrected -log(p-value) and directionality (blue= depleted, yellow= enriched) within each cancer type for Tregs, CD4$^+$ T cells, and CD8$^+$ T cells; stratified by p-values (high to low) for difference in Tregs. (**B**) Eosinophil, Treg, CD4$^+$ T cell, and CD8$^+$ T cell predictions for melanoma (SKCM, top) and colorectal cancer (COAD, bottom) for cases with eosinophil detection (EO+) or no eosinophil detection (EO^{Neg}). Adj p-values are from False Discovery Rate corrected paired t-test.
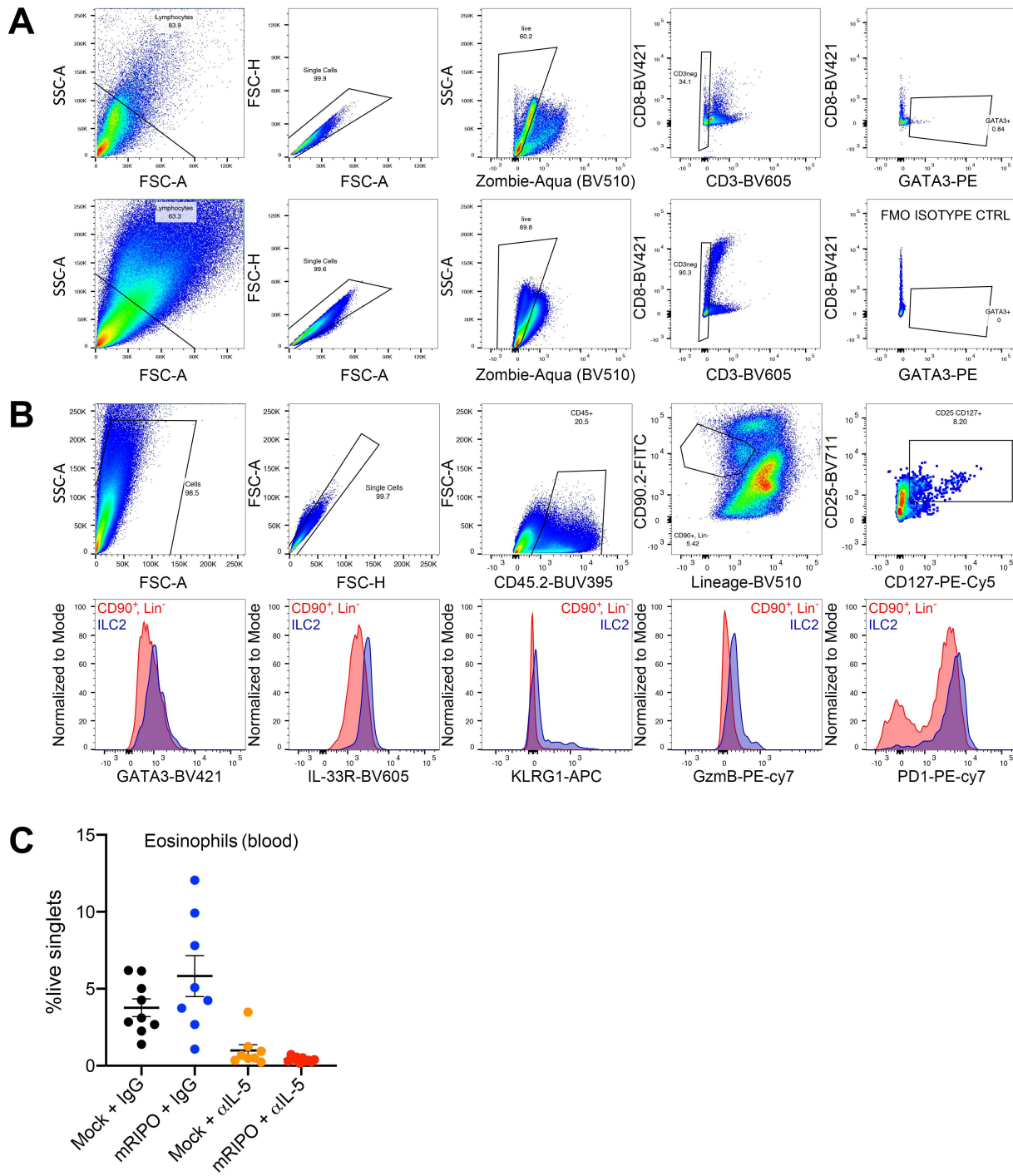
Supplementary Figure 13. (A) Gating strategy for %GATA3+ CD3^{Neg} cells presented in Figure 5C from prior experiments conducted in Figure 4. FMO= florescence minus one. **(B)** Gating strategy for ILC2s in Figures 5G and S10B, D (top), along with representative histograms showing ILC2 vs Lin$^-$CD90.2$^+$ cells (bottom). Lineage= Zombie Aqua (live dead), CD3, CD5, CD19, NK1.1, CD11c, CD11b, FCεRIα, γδTCR, αβTCR. **(C)** Blood eosinophil levels determined for the experiment presented in Figure 5D-G.

Supplementary Table 1. Details of antibodies used in this study.

Antigen	Flurophore	Vendor	RRID/Identifier
BCL6	PEcy7	Biolegend	AB_2566196
CCR3	BV421	Biolegend	AB_2565743
CD103	PE	BIolegend	catalog# 156904
CD11b	BV711	Biolegend	AB_2563310
CD11b	BV510	Biolegend	AB_2629529
CD11c	APC	Biolegend	AB_313779
CD11c	BV605	Biolegend	AB_2562415
CD11c	BV510	Biolegend	AB_2562016
CD127	PEcy5	Biolegend	AB_1937261
CD19	FITC	Biolegend	AB_2629813
CD19	BUV395	BD Biosciences	AB_2722495
CD19	BV510	Biolegend	AB_2562137
CD25	BV711	Biolegend	AB_2564130
CD3	APC	Biolegend	AB_2561456
CD3	FITC	Biolegend	AB_312661
CD3	BV510	Biolegend	AB_2562555
CD3	PE	Biolegend	AB_312663
CD4	FITC	Biolegend	AB_312713
CD40	BV605	BD Biosciences	AB_2742809
CD44	PEcy5	Biolegend	AB_312961
CD45.2	BUV395	BD Biosciences	AB_2738867
CD45.2	APCcy7	Biolegend	AB_830789
CD5	BV510	Biolegend	AB_2563930
CD69	BV605	Biolegend	AB_11203710
CD8	BV421	Biolegend	AB_11204079
CD8	FITC	Thermo-Fisher	AB_2538242
CD86	PEcy7	Biolegend	AB_493600
CD90.2	AF488	Biolegend	AB_492886
F4/80	PEcy5	Biolegend	AB_893482
FCgR	BV510	Biolegend	AB_2721324
FoxP3	PEcy5	Thermo-Fisher	AB_468806
GATA3	PE	Biolegend	AB_2562723
Granzyme B	PEcy7	Biolegend	AB_2728381
IA/IE (MHC-II)	BV786	Biolegend	AB_2565977
IFN-g	BV786	Biolegend	AB_2629667
IL33R/ST2	BV605	Biolegend	AB_2860703
IL5	PE	BD Biosciences	AB_395364
IRF4	PercpCy5.5	Biolegend	AB_2728482
KLRG1	APC	Biolegend	AB_10641560
LY6C	PercpCy5.5	Biolegend	AB_1659241
LY6G	PE	Biolegend	AB_1186099
NK1.1	BV421	Biolegend	AB_2562218
NK1.1	BV510	Biolegend	AB_2562217
PD1	PeCy7	Thermo-Fisher	AB_10853805
PD1	BV786	Biolegend	AB_2563680
PDL1	APC	Biolegend	AB_10612741
RORgT	BV786	BD Biosciences	AB_2738916
Siglec F	AF488	Biolegend	catalog# 155524
Tbet	BV711	Biolegend	AB_2715766
TCRb	BV510	Biolegend	AB_2562350
TCRg/d	BV510	Biolegend	AB_2563534
TIM3	BV711	Biolegend	AB_2716208
TNF	BV605	Biolegend	AB_11123912
TruStain FcX	N/A	Biolegend	AB_1574975

SUPPLEMENTARY METHODS:

Polio neutralizing antibody assay and ELISA. Polio neutralization assays were performed as previously described[9]. ELISA to measure anti-polio antibodies was performed using Maxisorp plates (Nunc) coated with $1x10^7$ pfu PVSRIPO; blocked in PBS + 2% BSA + 0.05% Tween-20 (Sigma-Aldrich); incubated with serially diluted sera (1:20, 1:100, 1:500) for 2h; followed by incubation with 1:30,000 protein-A conjugated HRP (Thermo-Fisher) diluted in PBS for 1h; and development using TMB substrate (Thermo-Fisher) followed by blocking the reaction with H2SO4 (Sigma-Aldrich). Absorbance (450nm) was measured using a Tecan Infinite pro plate reader. A similar procedure was used for detection of KLH antibodies and Tetanus-specific antibodies, coating plates at a concentration of 10 or 1µg/ml antigen, respectively.

Tumor homogenate TDLN culture cytokine measurements. Freshly harvested B16 tumors were mechanically homogenized in 1ml PBS. Samples were frozen at -80°C, thawed, and centrifuged (4,000xG for 10min) to remove solid debris prior to cytokine analysis. Fresh TDLNs (inguinal lymph nodes) were collected in 1ml RPMI-1640 (Gibco), crushed over a 70-micron cell strainer (Olympus Plastics) using a 3ml syringe plunger (BD Biosciences), and resuspended in RPMI-1640 containing 10% FBS. Resulting cell suspensions were plated in a U-bottom 96 well cell culture plate (Greiner Bio-One) at a density of $5x10^6$ and cultured at 37°C for 24 hours. Cell suspensions were frozen until cytokine measurements were performed. Mouse Anti-Virus and Mouse Th Legendplex kits (Biolegend) were used to determine indicated analyte concentrations per manufacturer instructions, using the manufacturer's analysis software to determine concentration. Cytokines without measurable concentrations above the lower limit of detection for more than 50% of the samples tested were excluded. For samples below the threshold, the threshold value was used.

Adoptive transfer studies and RNA sequencing of tumor infiltrating OT-I T cells. For adoptive transfer of $CD4^+$ T cells from polio or Tet immunized mice, spleens (two each) were harvested. Separately, hCD155-tg C57BL/6 mice were implanted with B16.F10.9[hCD155] tumors six days prior to splenocyte isolation. Spleens from immunized mice were crushed through a 70µm cell strainer in 3ml RPMI-1640. Resulting cell pellets were reconstituted in 2ml ACK red blood cell lysis buffer (Lonza) and incubated for 10 min at RT, followed by addition of 10ml RPMI and centrifugation.

CD4$^+$ T cells were negatively selected from single cell suspensions using the EasySep^{TM} CD4$^+$ T cell isolation kit (Stemcell Technologies) following the manufacturer's instructions. Two million CD4$^+$ T cells were injected intraperitoneally six days after B16^{hCD155} tumor implantation. Seven days after tumor implantation, recipient mice were treated with mock (DMEM) or mRIPO (1×10^7 pfu) and tumor growth was monitored. For adoptive transfer of OT-I x CD45.1 cells, spleens from OT-I x CD45.1 mice were harvested and processed to single cell suspensions as described above. OT-I splenocytes were treated with 10μg/ml SIINFEKL peptide (Invivogen) for 16 hours, washed in PBS, and then 2×10^6 OT-I splenocytes were transferred in 100μl i.p. For transfer of T cells from mice treated with recall antigen therapy, splenocytes were processed as described above and transferred to naïve recipients immediately following subcutaneous injection of B16.F10.9-OVA cells. For analysis of OT-I T cell transcriptomes after polio recall, mice immunized against polio (PVSRIPO, 1×10^7 pfu in Alhydrogel) 45 days (prime) and 30 days (boost) prior to B16-OVA tumor implantation received SIINFEKL-activated OT-I splenocytes as described above, and were treated with intratumor mock (PBS) or UVP 9 days after tumor implantation. Twelve days post-treatment tumors were dissociated and subjected to CD45.1 positive selection (MojoSort cell mouse CD45.1 selection kit, Biolegend) per the manufacturer's instructions. A subset of the isolated cells were used to confirm purity by flow cytometry for 7-AAD (Biolegend), CD45.2-BUV395, CD3-PE, CD8-BV421, CD4-FITC; the remaining cells were lysed in 200μl Trizol (Thermo-Fisher). Chloroform extracted RNA from Trizol samples (per manufacturer's instructions) was purified using the RNEasy kit (Qiagen, Inc.) and analyzed on a Hi-seq Illumini sequencer (150bp, PE) at Azenta Life Sciences. Transcripts were aligned with STAR (v2.7) to the GRCm38 mouse genome and differential expression analysis was performed using DESeq2 (v 1.34).

Flow cytometry antibody panels. The panels used in this study include the following antigen-specific antibodies or reagents (see Supplementary Table 1 for antibody sources): lineage panel 1: CD45.2-BUV395 and CD40-BV605, Zombie-Aqua Live/dead, NK1.1-BV421, CD11b-BV711, IA/IE-BV786, CD19-FITC, LY6G-PE, F4/80-PEcy5, CD86-PEcy7, CD3-APC; lineage panel 2: CD19-BUV395, 7-AAD, CD45.2-APC-Cy7, CD11b-BV711, LY6C-PerCP-Cy5.5, LY6G-PE, CD3-FITC, CD11c-APC; lineage panel 3: CD45.2-BUV395 and CD40-BV605, Zombie-Aqua Live/dead, NK1.1-BV421, CD11b-BV711, IA/IE-BV786, CD3/CD19-FITC, LY6G-PE, F4/80-

PEcy7, CD86-PEcy7, CD11c-APC; T cell panel: CD45.2-BUV395, Zombie-Aqua Live/dead, CD3-PE, CD4-FITC, CD8-BV421, CD69-BV605, PD1-PE-Cy7, TIM3-BV711, CD44-PE-Cy5; Intracellular staining T cell panel 1: CD45.2-BUV395, Zombie-Aqua Live/dead, CD3-APC, CD4-FITC, CD8-BV421, FoxP3-PE-Cy5, IFN-γ-BV786, TNF-BV605, Granzyme B-PE-Cy7; intracellular staining T cell panel 2: CD45.2-BUV395, Zombie-Aqua Live/dead, CD3-APC, CD4-FITC, CD8-BV42, FoxP3-PE-Cy5, Tbet-BV711, GATA3-PE, IRF4-PerCP-Cy5.5, RoRγT-BV786, and BCL6-PE-Cy7; OT-I T cell panels were accomplished using the three above T cell panels with exchange of CD45.2 for CD45.1-BUV395; Eosinophil panel: CD45.2-BUV395, CCR3-BV421, Zombie Aqua, CD3/CD19/NK1.1-BV510, CD11c-BV605, CD11b-BV711, IA/IE-BV786, Siglec F-AF488, Ly6C-PERCP-Cy5.5, CD103-PE, F4/80-PECy5, PD1-PEcy7, PD-L1-APC; and ILC2 panel: CD45.2-BUV395, Zombie Aqua, CD3/CD5/CD19/NK1.1/CD11c/CD11b/FCεRIa/γδTCR/αβTCR-BV510, ST-2(IL33R)-BV605, CD25-BV711, PD1-BV786, CD90.2-AF488, IL5-PE, CD127-PEcy5, Granzyme B-PECy7, KLRG1-APC.

Analysis of TRP2-MHC-class I specific CD8 T cells in B16 tumors and TDLNs. The day before harvest, Flex-T Biotin H2 K(b) TRP2 Monomers (SVYDFFVWL; Biolegend) were multimerized and conjugated with PE or BV421 streptavidin (both Biolegend) according to the manufacturer's instructions. Polio immunized mice bearing B16 tumors treated with mock or UVP in the presence or absence of CD4 depleting antibody (see main text) as described in corresponding figure legends were euthanized; tumors and TDLN (inguinal lymph node) were harvested and dissociated as described in the Materials and Methods section of the main text. After dissociation, single cell suspensions were stained with Zombie Aqua, followed by incubation with the SRC inhibitor Dasatinib (Tocris) in FACs buffer (10% FBS + PBS) at a concentration of 100nM for 30 minutes to prevent TCR internalization during multimer staining. Following incubation, samples were stained for 30min at 4°C using 2μl per sample of the prepared BV421 and PE bound TRP2-MHCclass I multimers. Surface staining antibodies were then used for staining (see Supplementary Table 1 for antibody information): CD45.2-BUV395, CD19-BV510, CD11b-BV510, CD3-BV605, TIM3-BV711, PD1-BV786, CD8a-FITC, and CD3-APC. Samples were incubated for 30 minutes at 4°C followed by washing in FACs buffer. Samples were then fixed and permeabilized using the FoxP3/Transcription Factor Staining Buffer Set (Thermo-Fisher), following manufacturer instructions, and stained with Granzyme B-PEcy7 overnight. Cells were washed and

Supplemental material

BMJ Publishing Group Limited (BMJ) disclaims all liability and responsibility arising from any reliance placed on this supplemental material which has been supplied by the author(s)

J Immunother Cancer

analyzed. Inguinal lymph nodes from non-tumor bearing mice were used to determine TRP2-MHC class I multimer bound CD8$^+$ T cells.

Associations of eosinophils with other cell types in human tumors and survival. CIBERSORT predicted cell type enrichment for each cancer type were obtained from Thorsson et al[37]. Within each cancer type, cases were sorted by eosinophil enrichment, and comparisons were performed between cases with eosinophil score = 0 (EO^{Neg}) vs eosinophil score >0 (EO+). Total CD4$^+$ T cells reflects the sum of the following scores: 'T cells CD4 Memory Activated' + 'T cells CD4 Memory Resting' + 'T cells CD4 Naïve' + 'T cells follicular helper.' For pan-cancer analyses mean enrichment values for each cell type were determined for EO^{Neg} and EO+ for comparison. Mean values from each cell type were scaled and centered within each cell type score across all samples (both EO^{Neg} and EO+), followed by subtracting normalized EO+ from EO^{Neg} values to to generate heatmaps in Fig S9B and Fig S10A. False discovery rate (Benjamini-Hochberg method) was used to adjust for multiple comparisons in Figs S9B and S10A. Hazard ratios and 95% confidence intervals of survival of patients in EO+ vs EO^{Neg} cohorts were determined using the Mantel-Haenszel test and statistical significance was determined using a Mantel-Cox log rank test.